bioRxiv preprint doi: https://doi.org/10.1101/491613; this version posted December 10, 2018. The copyright holder for this preprint (which was not certified by peer review) is the author/funder. All rights reserved. No reuse allowed without permission.

1 DENTATE GYRUS ACTIVIN SIGNALING MEDIATES THE ANTIDEPRESSANT
2 TREATMENT RESPONSE
3

4 Mark M. Gergues[1,2,*], Christine N. Yohn[1,*], Marjorie R. Levinstein[3], Benjamin A. Samuels[1#]
5
6
7 [1]Department of Psychology, Rutgers, The State University of New Jersey, New Brunswick, New
8 Jersey, United States of America
9 [2]Department of Neuroscience, University of California San Francisco, San Francisco, California,
10 United States of America
11 [3]Department of Neuroscience, University of Washington, Seattle, Washington, United States of
12 America
13
14 [*] These authors contributed equally
15 # Address correspondence to: ben.samuels@rutgers.edu
16
17
18
19
20 Keywords: depression, dentate gyrus, activin, fluoxetine, treatment resistance, antidepressant
21

bioRxiv preprint doi: https://doi.org/10.1101/491613; this version posted December 10, 2018. The copyright holder for this preprint (which was not certified by peer review) is the author/funder. All rights reserved. No reuse allowed without permission.

22 **ABSTRACT**

23 Antidepressants that target monoaminergic systems, such as selective serotonin reuptake
24 inhibitors (SSRIs), are widely used to treat neuropsychiatric disorders including major depressive
25 disorder, several different anxiety disorders, and obsessive-compulsive disorder. However, these
26 treatments are not ideal because only a subset of patients achieve remission. The reasons why
27 some individuals remit to antidepressant treatments while others do not are unknown. Here, we
28 developed a paradigm to assess antidepressant treatment resistance in mice. Treatment of mice
29 with either chronic corticosterone or chronic social defeat stress effectively induces increased
30 negative valence behaviors. Subsequent chronic treatment with the SSRI fluoxetine reverses
31 these behavioral changes in some, but not all, of the mice, permitting stratification into persistent
32 responders and non-responders to fluoxetine. We found several significant differences in
33 expression of Activin signaling-related genes between responders and non-responders to
34 fluoxetine in the dentate gyrus, a region that we recently reported is critical for the beneficial
35 behavioral effects of fluoxetine. Furthermore, enhancement of Activin signaling in the dentate
36 gyrus converted behavioral non-responders into responders to fluoxetine treatment more
37 effectively than commonly used adjunctive antidepressant treatments, while inhibition of Activin
38 signaling in the dentate gyrus converted responders into non-responders. Taken together, these
39 results demonstrate that the behavioral response to FLX can be bidirectionally modified via
40 targeted manipulations of the dentate gyrus and suggest that molecular- and neural circuit-based
41 modulations of dentate gyrus may provide a new therapeutic avenue for more effective
42 antidepressant treatments or adjunctive therapies.

43

44

bioRxiv preprint doi: https://doi.org/10.1101/491613; this version posted December 10, 2018. The copyright holder for this preprint (which was not certified by peer review) is the author/funder. All rights reserved. No reuse allowed without permission.

45 **INTRODUCTION**

46 Approximately 32-35 million adults in the US population (16%) experience an episode of
47 major depression in their lifetime[1], and commonly used treatments, such as selective serotonin
48 reuptake inhibitors (SSRIs), are not ideal since only a subset of patients (~33%) achieves
49 remission with initial treatment[2,3]. However, despite this large population of non-remitters, the
50 reasons why some individuals remit to antidepressant treatments while others do not remain
51 unknown. Given that SSRIs are widely used to treat not only major depressive disorder, but also
52 several anxiety disorders and obsessive-compulsive disorder, improving our understanding of the
53 basis of this treatment resistance is of paramount importance. One approach is to decipher the
54 neural circuitry and molecular mechanisms that underlie antidepressant treatment response and
55 resistance.

56 Several brain regions, including prefrontal and cingulate cortices, amygdala, thalamus,
57 hypothalamus, nucleus accumbens, and hippocampus are implicated in mood disorders through
58 imaging and postmortem studies[4,5]. Within the hippocampus, several preclinical studies in
59 rodents demonstrate that the dentate gyrus (DG) subfield is an essential component of the neural
60 circuitry mediating the antidepressant response. Serotonin 1A receptors on mature dentate gyrus
61 (DG) granule cells are critical mediators of the negative valence behavioral and the
62 neuroendocrine response to the SSRI fluoxetine[6]. Furthermore, chronic treatment with most
63 antidepressants (including SSRIs) stimulates adult neurogenesis in the dentate gyrus (DG)[7,8].
64 Chronic SSRI treatment increases proliferation of dividing neural precursor cells and promotes
65 maturation and integration of young adult born granule cells (abGCs) into the DG and ablation or
66 impairment of this neurogenic niche results in the loss of some antidepressant-mediated
67 behaviors[7-12]. Direct peptide infusions of brain-derived neurotrophic factor (BDNF), vascular
68 endothelial growth factor (VEGF), or Activin A, yield an antidepressant-like behavioral

bioRxiv preprint doi: https://doi.org/10.1101/491613; this version posted December 10, 2018. The copyright holder for this preprint (which was not certified by peer review) is the author/funder. All rights reserved. No reuse allowed without permission.

69 response[13-17]. Likewise, targeting entorhinal cortex projections to the DG yields an
70 antidepressant-like behavioral response[18]. Optogenetic and chemogenetic manipulations of
71 ventral DG granule cells demonstrate a role in anxiety-related behaviors and stress resilience[19-21].
72 Serotonin 1B receptors on cholecystokinin (CCK) inhibitory interneurons in the DG are also
73 essential for mediating the negative valence behavioral response to SSRI treatment[22]. Finally,
74 humans suffering from major depressive disorder have fewer DG GCs than controls and DG
75 volume is inversely correlated with the number of depressive episodes[23,24]. Taken together, all of
76 these data indicate that the DG is a principal component of the neural circuitry mediating the
77 antidepressant response. Therefore, both molecular and functional manipulations of the DG will
78 ultimately be important for determining the differences between remitters and non-remitters to
79 antidepressant treatment and may prove instructive for development of new augmentation
80 therapies.
81 Exposure of rodents to chronic stressful experiences can induce a long-lasting affective
82 state in which there are increases in negative valence behaviors. This negative affective state is
83 often associated with or described as an experimental system to study mood disorders. Several
84 highly distinct stress paradigms are commonly used for this purpose, including chronic mild
85 stress, chronic social defeat stress, and chronic administration of glucocorticoids[11,25-37].
86 Importantly, these stressed rodents can be treated with antidepressants to reverse the negative
87 valence behaviors and better understand the neural effects of antidepressants. Interestingly, we
88 have noticed that in the Novelty Suppressed Feeding (NSF) behavioral task, SSRI treatment only
89 reverses the effects of chronic glucocorticoid administration in a subset of mice, suggesting that
90 there may be responders and non-responders to antidepressant treatment[29,38]. Therefore, we
91 sought to better understand and characterize this potential treatment resistance phenotype and

bioRxiv preprint doi: https://doi.org/10.1101/491613; this version posted December 10, 2018. The copyright holder for this preprint (which was not certified by peer review) is the author/funder. All rights reserved. No reuse allowed without permission.

92 then to assess differences in the DG between responders and non-responders in order to

93 determine how to manipulate the DG to modify the response to antidepressant treatment.

bioRxiv preprint doi: https://doi.org/10.1101/491613; this version posted December 10, 2018. The copyright holder for this preprint (which was not certified by peer review) is the author/funder. All rights reserved. No reuse allowed without permission.

94 **RESULTS**
95
96 ***Behavioral Responders and Non-Responders to FLX treatment following CORT***
97 ***administration***

98 To better understand the potential treatment resistance phenotype following chronic stress
99 and antidepressant treatment, we began by exposing a cohort (n=70) of group housed 8-week-
100 old male C57BL/6J mice to chronic administration with either vehicle or corticosterone
101 (CORT, 5mg/kg/day via drinking water). Chronic CORT administration at this dosage induces
102 several negative valence behaviors, including increased latency to feed in NSF and decreased
103 open arm entries and duration in the elevated plus maze (EPM)[11]. We administered vehicle or
104 CORT for 4 weeks and then added either vehicle or the SSRI fluoxetine (FLX, Prozac,
105 18mg/kg/day) to the treatment paradigm for an additional 3 weeks (timeline of treatments in
106 Figure 1a). As expected, chronic CORT induced an increased latency to feed in NSF relative to
107 vehicle only treated mice (CORT+VEH vs VEH $p = 0.004$, logrank Mantel-Cox test with
108 Bonferroni correction) and coadministration of CORT and FLX significantly reduced latency to
109 feed relative to CORT treated mice indicative of an antidepressant response (CORT+FLX vs
110 CORT+VEH $p < 0.0001$, logrank Mantel-Cox with Bonferroni correction) (Figure 1b left).
111 However, closer inspection of the individual latencies of CORT+FLX mice demonstrated a
112 bimodal distribution (Figure 1b right), providing a potential basis for dividing mice into
113 responders and non-responders to FLX treatment groups. Importantly, all mice that received
114 FLX showed similar levels of FLX in their serum (Supplemental Figure 1). Furthermore, food
115 consumption in the home cage was similar among all mice (data not shown).

116 We next exposed the same cohort of C57BL/6J mice to EPM and then the forced swim test
117 (FST), which is a commonly used test of antidepressant efficacy. In the EPM, separate two-way

bioRxiv preprint doi: https://doi.org/10.1101/491613; this version posted December 10, 2018. The copyright holder for this preprint (which was not certified by peer review) is the author/funder. All rights reserved. No reuse allowed without permission.

118 ANOVAs revealed effects of CORT administration and FLX treatment in open arm entries
119 (CORT: $F_{(1,66)} = 9.69$, $p = 0.0027$, FLX: $F_{(1,66)} = 19.4$, $p < 0.0001$) and open arm duration
120 (CORT: $F_{(1,66)} = 10.34$, $p = 0.002$, FLX: $F_{(1,66)} = 15.42$, $p = 0.0002$) (Figure 1c small panels).
121 To investigate behavioral differences between CORT only treated mice, NSF-defined
122 CORT+FLX responders, and non-responders in the EPM, we next used one-way ANOVAs and
123 found significant differences in open arm entries ($F_{(2,36)} = 33.24$, $p < 0.001$) and duration ($F_{(2,36)}$
124 $= 36.54$, $p < 0.001$) (Figure 1c large panels), with Bonferroni-corrected post hoc tests
125 demonstrating that responders had significantly increased open arm entries and duration
126 relative to vehicle treated mice and non-responders (entries and duration: CORT+VEH vs
127 CORT+FLX-R and CORT+FLX-R vs CORT+FLX-NR, all $p < 0.001$). Non-responders did not
128 show any significant differences relative to vehicle treated mice (entries and duration:
129 CORT+VEH vs CORT+FLX-NR, $p > 0.999$ for both). These data suggest that FLX response
130 status is conserved across the NSF and EPM. Similarly, in the FST, a two-way ANOVA
131 revealed effects of both CORT administration ($F_{(1,66)} = 4.83$, $p = 0.031$) and FLX treatment
132 ($F_{(1,66)} = 22.24$, $p < 0.0001$) (Figure 1d small panel) on immobility over the last four minutes of
133 the six minute test. A separate one-way ANOVA demonstrated significant differences in
134 immobility ($F_{(2,36)} = 21.02$, $p < 0.001$) (Figure 1d large panel), with Bonferroni-corrected post
135 hoc tests demonstrating that responders had significantly decreased immobility relative to
136 vehicle treated mice and non-responders (CORT+VEH vs CORT+FLX-R and CORT+FLX-R
137 vs CORT+FLX-NR, both $p < 0.001$). Non-responders did not show any significant differences
138 relative to vehicle treated mice in the FST (CORT+VEH vs CORT+FLX-NR, $p > 0.999$).
139 Taken together, these data suggest that FLX response status across NSF, EPM, and FST is
140 conserved in CORT-treated mice.

bioRxiv preprint doi: https://doi.org/10.1101/491613; this version posted December 10, 2018. The copyright holder for this preprint (which was not certified by peer review) is the author/funder. All rights reserved. No reuse allowed without permission.

141 A negative affect index was next used to assess the behavior of this cohort of mice
142 across EPM, NSF, and FST as previously described[39,40] (Figure 1e). Briefly, z-scores were
143 calculated in each behavioral test (EPM, NSF, FST) by normalizing individual animals against
144 control group averages and standard deviation. Each behavioral test z-score was then averaged
145 for each animal and group averages were calculated. The score shows a more comprehensive
146 analysis of behavior across multiple behavioral modalities where a score above zero represents
147 an animal that shows low open arm entries and time in the EPM, high immobility times in the
148 FST, and longer latency to feed in the NSF task relative to control. A two-way ANOVA
149 revealed significant effects of CORT ($F_{(1,66)} = 6.41$, $p = 0.013$) and FLX ($F_{(1,66)} = 12$, $p =$
150 0.0009) treatment on the negative affect index (Figure 1e small panel). A separate one-way
151 ANOVA demonstrated significant differences in negative affect index ($F_{(2,36)} = 261.4$, $p <$
152 0.001), with Bonferroni-corrected post hoc tests demonstrating that responders had a
153 significantly decreased negative affect index relative to vehicle treated mice and non-
154 responders (CORT+VEH vs CORT+FLX-R and CORT+FLX-R vs CORT+FLX-NR, both $p <$
155 0.001) (Figure 1e large panel). Non-responders did not have a significantly different negative
156 affect index than vehicle treated mice (CORT+VEH vs CORT+FLX-NR, $p > 0.999$).
157 We next directly assessed the relationship between NSF latency to feed and behavioral
158 performance in the EPM and FST among CORT+FLX treated mice. Significant relationships
159 emerged between NSF latency to feed and open arm time (Pearson $r = -0.786$, $p < 0.0001$,
160 Figure 1f), as well as NSF latency to feed and immobility duration (Pearson $r = 0.773$, $p <$
161 0.0001). To characterize these relationships further we ran two separate linear regressions, with
162 NSF latency and open arm time having a linear regression line ($y = -6.02x + 780$, $F_{(1,21)} =$

bioRxiv preprint doi: https://doi.org/10.1101/491613; this version posted December 10, 2018. The copyright holder for this preprint (which was not certified by peer review) is the author/funder. All rights reserved. No reuse allowed without permission.

163 33.9, $p < 0.0001$), and FST linear regression line ($y = 4.63x - 415$, $F_{(1,21)} = 31.1$, $p < 0.0001$)
164 (Figure 1f) .
165 Finally, we wanted to assess whether the responder and non-responder phenotypes persisted
166 across several months (Figure 1g). To this end, we exposed a new cohort of C57BL/6J mice to
167 CORT+FLX as in Figure 1a, and then assessed behavior in NSF. Similar to the cohort in Figure
168 1b, the CORT+FLX mice displayed a bimodal distribution of latencies to feed. These mice then
169 remained on CORT+FLX and were retested several times in the NSF. Importantly, the
170 responder vs non-responder behavioral distinction persists for at least 6 months (repeated
171 measures ANOVA reveals significant effect of response status [$F_{(1, 22)} = 4350$, $p < 0.0001$], but
172 not time [$F_{(3, 66)} = 0.255$, $p = 0.8573$]). Therefore, the CORT+FLX paradigm permits definition
173 of persistent responders and non-responders to FLX treatment and potentially allows for
174 additional manipulations in attempts to convert non-responders into responders.
175
176 ***Dentate Gyrus mRNA expression of Activin signaling components correlates with behavioral***
177 ***response to FLX treatment following CORT administration***
178 We previously published a preliminary microarray study assessing DG gene expression
179 in CORT+VEH and CORT+FLX-treated mice[38]. However, when we looked at CORT+FLX
180 responders vs non-responders in these microarray data, pathway analyses suggested that there
181 were differences in multiple components of DG Activin signaling. We were particularly
182 interested in further analyzing this pathway because previous reports have demonstrated that
183 some Activin signaling components are altered in DG by antidepressant treatment and that
184 acute Activin A infusions have antidepressant-like effects in FST[16,17].

bioRxiv preprint doi: https://doi.org/10.1101/491613; this version posted December 10, 2018. The copyright holder for this preprint (which was not certified by peer review) is the author/funder. All rights reserved. No reuse allowed without permission.

185 To fully characterize Activin signaling in DG of responders and non-responders, we
186 prepared a new cohort of vehicle, CORT+VEH, and CORT+FLX treated mice (behavioral data
187 in Supplemental Figure 2), and prepared DG RNA following behavioral testing. Two-way
188 ANOVAs revealed significant effects of FLX treatment on DG expression of Activin A (Figure
189 2a middle panel, $F_{(1,62)} = 85.51$, $p < 0.0001$), the Activin receptors acvr1a (Figure 2b middle
190 panel, $F_{(1,62)} = 28.15$, $p < 0.0001$) and acvr1c (Figure 2d middle panel, $F_{(1,62)} = 35.37$, $p <$
191 0.0001), and the intracellular signaling protein smad3 (Figure 2f middle panel, $F_{(1,62)} = 45.19$, p
192 < 0.0001) and of CORT administration on Activin A (Figure 2a middle panel, $F_{(1,62)} = 5.01$, $p =$
193 0.0288) and acvr1b (Figure 2c middle panel, $F_{(1,62)} = 7.285$, $p = 0.009$). Separate one-way
194 ANOVAs were next used to compare DG expression of these genes in CORT+FLX responders,
195 CORT+FLX non-responders, and CORT+VEH mice. These analyses revealed significant
196 group differences in Activin A (Figure 2a left panel, $F_{(2,36)} = 81.68$, $p < 0.001$), acvr1a (Figure
197 2b left panel, $F_{(2,36)} = 34.7$, $p < 0.001$), acvr1c (Figure 2d left panel, $F_{(2,36)} = 56.97$, $p < 0.001$),
198 smad2 (Figure 2e left panel, $F_{(2,36)} = 23.73$, $p < 0.001$), and smad3 (Figure 2f left panel, $F_{(2,36)} =$
199 72.33, $p < 0.001$). Interestingly, CORT+FLX responders showed increased expression of
200 Activin A (Figure 2a), acvr1a (Figure 2b), acvr1c (Figure 2d), and smad3 (Figure 2f) ($p < 0.001$
201 for all, Bonferroni corrected) relative to CORT only treated mice and non-responders to
202 CORT+FLX. When comparing CORT+FLX non-responders to CORT+VEH mice, we found a
203 significant difference in activin A ($p = 0.047$, Bonferroni corrected) and smad2 expression ($p <$
204 0.001, Bonferroni corrected), but not in acvr1a, acvr1b, acvr1c, or smad3 expression (all $p >$
205 0.999, Bonferroni corrected). Finally, we directly compared NSF latency to feed with DG
206 expression of these genes. Significant relationships emerged between NSF latency to feed and
207 expression of activin A (Pearson $r = -0.817$, $p < 0.0001$), with linear regression line ($y =$

bioRxiv preprint doi: https://doi.org/10.1101/491613; this version posted December 10, 2018. The copyright holder for this preprint (which was not certified by peer review) is the author/funder. All rights reserved. No reuse allowed without permission.

208 $-3.23x + 2480$, $F_{(1,23)} = 46.2$, $p < 0.0001$) (Figure 2a right panel), acvr1a (Pearson $r = -0.76$, p
209 < 0.0001), with linear regression line ($y = -0.219x + 243$, $F_{(1,25)} = 31.5$, $p < 0.0001$) (Figure
210 2b right panel), acvr1c (Pearson $r = -0.815$, $p < 0.0001$), with linear regression line ($y =$
211 $-0.271x + 269$, $F_{(1,23)} = 49.9$, $p < 0.0001$) (Figure 2d right panel), smad2 (Pearson $r = 0.727$,
212 $p < 0.0001$), with linear regression line ($y = 0.108x + 69.3$, $F_{(1,23)} = 49.9$, $p < 0.0001$) (Figure
213 2e right panel), and smad3 (Pearson $r = -0.858$, $p < 0.0001$), with linear regression line ($y =$
214 $-0.221x + 240$, $F_{(1,23)} = 49.9$, $p < 0.0001$) (Figure 2f right panel). Taken together, all of these
215 data demonstrate that DG Activin signaling is significantly different between responders and
216 non-responders to FLX treatment.
217
218 ***Responders and Non-Responders to FLX treatment following chronic social defeat stress***
219 ***replicate the behavioral and DG Activin signaling expression data from the CORT***
220 ***administration paradigm***
221 To confirm that these effects on behavior and Activin signaling were due to differential
222 responses to FLX treatment and not a direct or secondary effect of CORT administration, we
223 next repeated these experiments using a distinct chronic stress paradigm. Chronic social defeat
224 stress (CSDS) is a widely used stress paradigm that involves exposing mice to multiple daily
225 defeats by a conspecific from a larger, more aggressive strain. To this end, we exposed a large
226 cohort (n=125) of 8-week-old male C57BL/6J mice to 10 days of either control or CSDS by
227 CD1 male mice prescreened for aggressive behavior (timeline in Figure 3a). The C57BL/6J
228 mice exposed to CSDS interacted with CD1 aggressors for 5 minutes per day and then were
229 cohoused with the CD1 aggressors separated by a transparent divider for further sensory
230 exposure. Following the 10 days of control or CSDS, the C57BL/6J mice were next exposed to

bioRxiv preprint doi: https://doi.org/10.1101/491613; this version posted December 10, 2018. The copyright holder for this preprint (which was not certified by peer review) is the author/funder. All rights reserved. No reuse allowed without permission.

231 a social interaction test, which indicated that n=35 of the CSDS exposed mice were susceptible
232 (SUS) to the CSDS (Supplemental Figure 3). Control and SUS mice were next administered
233 either VEH or FLX (18mg/kg/day) for 3 weeks and then exposed to a series of negative
234 behavior valence tests. Similar to CORT, SUS mice had an increased latency to feed in NSF
235 relative to control (SUS+VEH vs VEH, $p = 0.0003$, logrank Mantel-Cox test with Bonferroni
236 correction) (Figure 3b left) and administration of FLX to SUS mice significantly reduced
237 latency to feed (SUS+FLX vs SUS+VEH, $p < 0.0001$, logrank Mantel-Cox test with Bonferroni
238 correction). Interestingly, similar to CORT, the individual latencies of the SUS+FLX mice
239 showed a bimodal distribution indicative of responders and non-responders to FLX treatment
240 (Figure 3b right).

241 The same cohort of mice were next exposed to EPM and FST, and two-way ANOVAs
242 revealed significant effects of FLX treatment for EPM open arm entries ($F_{(1,67)} = 14.6$, $p =$
243 0.0003) (Figure 3c small panel), EPM open arm duration ($F_{(1,67)} = 13.35$, $p = 0.0005$) (Figure
244 3c small panel), and FST immobility ($F_{(1,67)} = 14.68$, $p = 0.00030$) (Figure 3d small panel) and
245 of CSDS on EPM open arm duration ($F_{(1,67)} = 6.993$, $p = 0.0102$) (Figure 3c small panel).
246 Subsequent one-way ANOVAs revealed significant differences in EPM open arm entries
247 ($F_{(2,32)} = 20.17$, $p < 0.001$) (Figure 3c large panel), EPM open arm duration ($F_{(2,32)} = 19.12$, $p <$
248 0.001) (Figure 3c large panel), and FST immobility ($F_{(2,32)} = 23.34$, $p < 0.001$) (Figure 3d large
249 panel), with SUS+FLX responders showing increased EPM open arm entries and duration and
250 decreased FST immobility relative to SUS+FLX non-responders and SUS+VEH mice ($p <$
251 0.001 for all, Bonferroni corrected). SUS+FLX non-responders were not significantly different
252 than SUS+VEH mice in EPM open arm entries, EPM open arm duration, and FST immobility
253 ($p > 0.999$ for all, Bonferroni corrected). A two-way ANOVA assessing negative affect index

bioRxiv preprint doi: https://doi.org/10.1101/491613; this version posted December 10, 2018. The copyright holder for this preprint (which was not certified by peer review) is the author/funder. All rights reserved. No reuse allowed without permission.

254 in this cohort of mice demonstrated a significant effect of FLX treatment ($F_{(1,67)} = 18.8$, $p <$
255 0.0001) (Figure 3e small panel). The subsequent one-way ANOVA found significant group
256 differences ($F_{(2,32)} = 64.66$, $p < 0.001$) (Figure 3e large panel), with SUS+FLX responders
257 showing a decreased negative affect index relative to SUS+VEH and SUS+FLX non-
258 responders ($p < 0.001$ for both, Bonferroni corrected). SUS+FLX non-responders were not
259 significantly different than SUS+VEH mice ($p > 0.999$, Bonferroni corrected). Significant
260 relationships also emerged when we directly compared NSF latency to feed to EPM open arm
261 duration (Pearson $r = -0.723$, $p = 0.0007$), with linear regression line ($y = -4.05x + 641$,
262 $F_{(1,16)} = 17.5$, $p = 0.0007$), and to FST immobility (Pearson $r = 0.864$, $p < 0.0001$), with linear
263 regression line ($y = 4.22x - 302$, $F_{(1,16)} = 47.2$, $p < 0.0001$) (Figure 3f). Taken together, these
264 data replicate the CORT behavioral data and demonstrate that FLX response status across NSF,
265 EPM, and FST is conserved in mice susceptible to CSDS.
266 We next assessed mRNA expression of Activin signaling components in the DG of the
267 CSDS cohort of mice. Two-way ANOVAs revealed significant effects of FLX treatment on DG
268 expression of Activin A (Figure 4a middle panel, $F_{(1,26)} = 37.45$, $p < 0.0001$), acvr1a (Figure 4b
269 middle panel, $F_{(1,26)} = 7.717$, $p = 0.0127$), acvr1c (Figure 4d middle panel, $F_{(1,26)} = 15.58$, $p =$
270 0.0005), and smad3 (Figure 4f middle panel, $F_{(1,26)} = 12.64$, $p = 0.0015$) and of CSDS on
271 acvr1b (Figure 4c middle panel, $F_{(1,26)} = 5.808$, $p = 0.023$). Subsequent one-way ANOVAs
272 found significant group differences for Activin A (Figure 4a left panel, $F_{(2,15)} = 54.65$, $p <$
273 0.001), acvr1a (Figure 4b left panel, $F_{(2,15)} = 9.82$, $p = 0.002$), acvr1b (Figure 4c left panel,
274 $F_{(2,15)} = 3.78$, $p = 0.047$), acvr1c (Figure 4d left panel, $F_{(2,15)} = 16.24$, $p < 0.001$), smad2 (Figure
275 4e left panel, $F_{(2,15)} = 3.769$, $p = 0.047$), and smad3 (Figure 4f left panel, $F_{(2,15)} = 23.38$, $p <$
276 0.001). Interestingly, SUS+FLX responders showed increased expression of Activin A (Figure

bioRxiv preprint doi: https://doi.org/10.1101/491613; this version posted December 10, 2018. The copyright holder for this preprint (which was not certified by peer review) is the author/funder. All rights reserved. No reuse allowed without permission.

277 4a), acvr1a (Figure 4b, SUS+VEH vs SUS+FLX-R ($p = 0.004$), SUS+FLX-R VS SUS+FLX-
278 NR ($p = 0.006$)), acvr1c (Figure 4d), and smad3 (Figure 4f) (all Bonferroni corrected, $p < 0.001$
279 for all except acvr1a) relative to SUS+VEH mice and SUS+FLX non-responders. By contrast,
280 similar to CORT, expression of acvr1a, acvr1c, and smad3 were not significantly different
281 between SUS+FLX non-responders and SUS+VEH mice ($p > 0.999$ for all, Bonferroni
282 corrected). Activin A expression was significantly increased in SUS+FLX non-responders
283 relative to SUS+VEH mice ($p = 0.035$, Bonferroni corrected).

284 Finally, we directly compared NSF latency to feed with DG expression of these genes in
285 responders and non-responders. Significant relationships emerged between NSF latency to feed
286 and expression of activin A (Pearson $r = -0.900$, $p < 0.0001$), with linear regression line ($y =$
287 $-3.70x + 2920$, $F_{(1,10)} = 42.5$, $p < 0.0001$) (Figure 4a right panel), acvr1a (Pearson $r = -0.765$,
288 $p = 0.0038$), with linear regression line ($y = -0.145x + 189$, $F_{(1,10)} = 14.1$, $p = 0.0038$) (Figure
289 4b right panel), acvr1c (Pearson $r = -0.848$, $p = 0.0005$), with linear regression line ($y =$
290 $-0.278x + 259$, $F_{(1,10} = 25.7$, $p = 0.0005$) (Figure 4d right panel), and smad3 (Pearson $r = -$
291 0.832, $p = 0.0008$), with linear regression line ($y = -0.261x + 263$, $F_{(1,10)} = 22.4$, $p = 0.0008$)
292 (Figure 4f right panel). Taken together, these data replicate the CORT Activin data and
293 demonstrate that DG Activin signaling is significantly different between responders and non-
294 responders to FLX treatment. Furthermore, in two distinct stress paradigms, FLX response
295 status is conserved across behavior and DG Activin signaling.

296

297 ***Chronic Activin A infusions into DG convert FLX non-responders into responders***

298 Since our gene expression data indicate that several components of DG Activin signaling,
299 including Activin A itself, are decreased in FLX non-responders relative to responders, we

bioRxiv preprint doi: https://doi.org/10.1101/491613; this version posted December 10, 2018. The copyright holder for this preprint (which was not certified by peer review) is the author/funder. All rights reserved. No reuse allowed without permission.

300 wanted to test whether this altered signaling underlies the lack of behavioral response to FLX.
301 Acute Activin A infusions directly into DG yield an antidepressant-like response in FST[16,17], so
302 we reasoned that development of a chronic Activin A infusion paradigm into DG could
303 potentially convert non-responders to FLX into responders. Since CORT+FLX response status
304 persists for at least six months, we exposed a large cohort of C57BL/6J mice to CORT+FLX,
305 and then non-responders (n=36) received bilateral cannula implants and were infused once
306 daily for two weeks with either vehicle (0.1% BSA), Activin A peptide (1.0 μg per hemisphere)
307 into DG, or Activin A peptide (1.0 μg per hemisphere) into CA1 (timeline in Figure 5a). These
308 mice were then exposed to NSF, EPM, and FST. Remarkably, CORT+FLX non-responders that
309 received chronic Activin A infusions into DG had reduced latency to eat in the NSF relative to
310 non-responders that received vehicle ($p < 0.0001$, logrank Mantel-Cox test with Bonferroni
311 correction) or chronic Activin A infusions into CA1 ($p < 0.0001$, logrank Mantel-Cox test with
312 Bonferroni correction) (Figure 5b). Closer inspection of individual latencies demonstrated that
313 all CORT+FLX non-responders that received DG Activin A infusions were converted into
314 responders in the NSF. Group differences were also observed in the EPM for open arm entries
315 ($F_{(2,33)} = 31.6$, $p < 0.0001$, Figure 5c) and duration ($F_{(2,33)} = 58.9$, $p < 0.0001$, Figure 5c) and in
316 the FST for immobility ($F_{(2,33)} = 57.4$, $p < 0.0001$, Figure 5d). CORT+FLX non-responders that
317 received DG Activin A infusions had increased open arm entries and duration and decreased
318 immobility relative to non-responders that received vehicle ($p < 0.0001$ for all, Bonferroni
319 corrected) or chronic Activin A infusions into CA1 ($p < 0.0001$ for all, Bonferroni corrected).
320 These data indicate that non-responders to CORT+FLX were converted into responders in
321 NSF, EPM, and FST. The negative affect index also demonstrated group differences ($F_{(2,33)} =$
322 647, $p < 0.0001$), with CORT+FLX non-responders that received DG Activin A infusions

bioRxiv preprint doi: https://doi.org/10.1101/491613; this version posted December 10, 2018. The copyright holder for this preprint (which was not certified by peer review) is the author/funder. All rights reserved. No reuse allowed without permission.

323 showing reduced negative affect relative to CORT+FLX non-responders that received vehicle
324 or Activin A infusions into CA1 ($p < 0.0001$ for both, Bonferroni corrected). Significant
325 relationships also emerged when we directly compared NSF latency to feed to EPM open arm
326 duration (Pearson $r = -0.873$, $p < 0.0001$), with linear regression line ($y = -5.81x - 864$,
327 $F_{(1,34)} = 109$, $p < 0.0001$), and to FST immobility (Pearson $r = 0.891$, $p < 0.0001$), with linear
328 regression line ($y = 3.77x - 160$, $F_{(1,34)} = 131$, $p < 0.0001$) (Figure 5f). Taken together, these
329 data demonstrate that supplementing Activin signaling in DG can convert FLX non-responders
330 into responders across NSF, EPM, and FST.
331
332 ***Inhibition of Activin signaling in DG converts FLX responders into non-responders***
333 Since chronic Activin A infusions into DG can convert FLX non-responders into
334 responders, we next wanted to test whether DG Activin signaling was necessary for the
335 behavioral response to FLX. Specifically, we sought to determine whether inhibition of Activin
336 signaling in DG converts FLX responders into non-responders. Inhibin is an endogenously
337 occurring protein complex that has nearly opposite biological effects to Activin[41]. Inhibin binds
338 directly to Activin receptor complexes, where Activin and Inhibin act as mutual antagonists to
339 each other[41]. Therefore, a cohort of C57BL/6J CORT+FLX responders (n=36) received
340 bilateral cannula implants and were infused once daily for two weeks with either vehicle (0.1%
341 BSA), Inhibin A peptide (1.0 µg per hemisphere) into DG, or Inhibin A peptide (1.0 µg per
342 hemisphere) into CA1 (timeline in Figure 6a). These mice were then exposed to NSF, EPM,
343 and FST. Excitingly, CORT+FLX responders that received chronic Inhibin A infusions into
344 DG had increased latency to eat in the NSF relative to non-responders that received vehicle (p
345 < 0.0001, logrank Mantel-Cox test with Bonferroni correction) or chronic Inhibin A infusions

bioRxiv preprint doi: https://doi.org/10.1101/491613; this version posted December 10, 2018. The copyright holder for this preprint (which was not certified by peer review) is the author/funder. All rights reserved. No reuse allowed without permission.

346 into CA1 ($p < 0.0001$, logrank Mantel-Cox test with Bonferroni correction) (Figure 6b). Group
347 differences were also observed in the EPM for open arm entries ($F_{(2,33)} = 12.9$, $p < 0.0001$,
348 Figure 6c) and duration ($F_{(2,33)} = 24.1$, $p < 0.0001$, Figure 6c) and in the FST for immobility
349 ($F_{(2,33)} = 39.4$, $p < 0.0001$, Figure 6d). CORT+FLX responders that received DG Inhibin A
350 infusions had decreased open arm entries and duration and increased immobility relative to
351 responders that received vehicle ($p = 0.0003$ for open arm entries, $p < 0.0001$ for open arm
352 duration and immobility, Bonferroni corrected) or chronic Inhibin A infusions into CA1 ($p =$
353 0.0003 for open arm entries, $p < 0.0001$ for open arm duration and immobility, Bonferroni
354 corrected). The negative affect index also demonstrated group differences ($F_{(2,33)} = 120$, $p <$
355 0.0001) (Figure 6e), with CORT+FLX responders that received DG Inhibin A infusions
356 showing increased negative affect relative to CORT+FLX responders that received vehicle or
357 Inhibin A infusions into CA1 ($p < 0.0001$ for both, Bonferroni corrected). Significant
358 relationships also emerged when we directly compared NSF latency to feed to EPM open arm
359 duration (Pearson $r = -0.776$, $p < 0.0001$), with linear regression line ($y = -5.99x - 748$,
360 $F_{(1,34)} = 51.3$, $p < 0.0001$), and to FST immobility (Pearson $r = 0.864$, $p < 0.0001$), with linear
361 regression line ($y = 4.46x - 391$, $F_{(1,34)} = 100$, $p < 0.0001$) (Figure 6f). Taken together, these
362 data demonstrate that Activin signaling in the DG is necessary for the behavioral effects of
363 FLX treatment as directly inhibiting Activin signaling in DG converts FLX responders into
364 non-responders across NSF, EPM, and FST. Furthermore, these data demonstrate that FLX
365 behavioral response status can be bidirectionally modified by manipulating DG Activin
366 signaling.
367

bioRxiv preprint doi: https://doi.org/10.1101/491613; this version posted December 10, 2018. The copyright holder for this preprint (which was not certified by peer review) is the author/funder. All rights reserved. No reuse allowed without permission.

368 ***Coinfusion of Activin A and Inhibin A into Non-Responders blocks the effects of Activin A on***
369 ***behavior***

370 To confirm that the effects of chronic DG Activin A infusions into CORT+FLX non-
371 responders were directly due to manipulation of Activin signaling as opposed to an off-target
372 effect, we next assessed whether chronic coinfusion of Inhibin A and Activin A blocked the
373 behavioral effects seen with Activin A alone. To this end, a cohort of C57BL/6J CORT+FLX
374 non-responders (n=48) received bilateral cannula implants and were infused once daily for two
375 weeks with either vehicle (0.1% BSA), Activin A peptide into DG (1.0 μg per hemisphere),
376 Inhibin A peptide (1.0 μg per hemisphere) into DG, or both Activin A and Inhibin A peptides
377 (1.0 μg of each per hemisphere) into DG (timeline in Figure 7a). These mice were then exposed
378 to NSF, EPM, and FST. In the NSF, chronic DG Activin A infusions into CORT+FLX non-
379 responders decreased latency to eat relative to vehicle, Inhibin A, and Activin A+Inhibin
380 infusions ($p < 0.0001$ for all, logrank Mantel-Cox test with Bonferroni correction) (Figure 7b).
381 Activin A+Inhibin A coinfusions were not significantly different than vehicle ($p = 0.129$, log-
382 rank Mantel-Cox test with Bonferroni correction) or Inhibin A ($p = 0.031$, log-rank Mantel-Cox
383 test not significant with Bonferroni correction). Group differences were also observed in the
384 EPM for open arm entries ($F_{(3,44)} = 27.3$, $p < 0.0001$, Figure 7c) and duration ($F_{(3,44)} = 34$, $p <$
385 0.0001, Figure 7c) and in the FST for immobility ($F_{(3,44)} = 48.2$, $p < 0.0001$) (Figure 7d).
386 CORT+FLX non-responders that received DG Activin A had increased open arm entries and
387 duration and decreased immobility relative to responders that received vehicle, Inhibin A, or
388 Activin A+Inhibin infusions ($p < 0.0001$ for all, Bonferroni-corrected). Activin A+Inhibin
389 coinfusions were not significantly different than vehicle or Inhibin A for EPM open arm
390 entries, open arm duration, or FST immobility ($p > 0.9999$ for all, Bonferroni corrected). The

bioRxiv preprint doi: https://doi.org/10.1101/491613; this version posted December 10, 2018. The copyright holder for this preprint (which was not certified by peer review) is the author/funder. All rights reserved. No reuse allowed without permission.

391 negative affect index also demonstrated group differences ($F_{(3,44)} = 538$, $p < 0.0001$) (Figure
392 7e), with CORT+FLX non-responders that received DG Activin A infusions showing decreased
393 negative affect relative to vehicle, Inhibin A, and Activin A+Inhibin infusions ($p < 0.0001$ for
394 all, Bonferroni corrected). Significant relationships also emerged when we directly compared
395 NSF latency to feed to EPM open arm duration (Pearson $r = -0.821$, $p < 0.0001$), with linear
396 regression line ($y = -5.23x - 826$, $F_{(1,46)} = 95$, $p < 0.0001$), and to FST immobility (Pearson r
397 $= 0.863$, $p < 0.0001$), with linear regression line ($y = 3.67x - 139$, $F_{(1,46)} = 135$, $p < 0.0001$)
398 (Figure 7f). Taken together, these data demonstrate that coinfusion of Inhibin A blocks the
399 ability of chronic DG Activin A infusions to convert FLX non-responders into responders
400 across NSF, EPM, and FST, and further suggests that the effects of Activin A infusions are
401 mediated through downstream Activin signaling.
402
403 ***Activin A infusions into DG are a more effective augmentation therapy than commonly used***
404 ***second-line treatments***
405 When human patients do not remit to initial antidepressant therapy, they are usually
406 switched to a new antidepressant. For example, in the large NIMH funded STAR*D study[2],
407 patients were first treated with citalopram (Celexa, a SSRI). Approximately 33% were found to
408 display remission of depression symptoms. The 67% that did not remit were then subdivided
409 into several groups and switched to either sertraline (Zoloft, a SSRI), bupropion (Wellbutrin, a
410 norepinephrine/dopamine reuptake inhibitor), or venlafaxine (Effexor, a
411 serotonin/norepinephrine reuptake inhibitor). Other groups either remained on citalopram and
412 were augmented with bupropion or received other treatments. Our data suggests that chronic
413 DG Activin A infusions are a very effective augmentation strategy for non-responders to FLX

bioRxiv preprint doi: https://doi.org/10.1101/491613; this version posted December 10, 2018. The copyright holder for this preprint (which was not certified by peer review) is the author/funder. All rights reserved. No reuse allowed without permission.

414 treatment. Therefore, we next wanted to assess whether switching mice from FLX to other
415 antidepressants or augmenting FLX with other antidepressants is as effective in converting non-
416 responders into responders as augmenting FLX with Activin A infusions into DG. To this end
417 we exposed a large cohort (n=250) of C57BL/6J mice to chronic CORT+FLX and then
418 assessed their behavior in NSF, where we found that n=79 were non-responders to FLX
419 treatment. Two weeks later, we cannulated all 79 FLX non-responders to bilaterally target the
420 DG and then housed the mice two per cage with a divider (timeline of experiment in Figure 8a).
421 One week after cannulation, we subdivided these non-responders into 6 groups of mice (n=12-
422 14 per group). Two groups remained on FLX, one group was switched to sertraline (SER,
423 10mg/kg/day)[42], one group was switched to bupropion (BUP, 10mg/kg/day)[43], one group was
424 switched to venlafaxine (VEN, 20mg/kg/day)[44], and the remaining group remained on FLX but
425 also began receiving bupropion (FLX+BUP, 10mg/kg/day of BUP). Then, one week after the
426 groups were formed, we began bilateral infusions. One of the two groups that remained on FLX
427 alone received Activin A infusions, while the other five groups received vehicle infusions.
428 Infusions were given once per day (over a time course of 15 minutes per hemisphere) for two
429 weeks. We then retested these six groups of mice in NSF (Figure 8b). The mice that remained
430 on FLX only and received vehicle infusions remained non-responders. Consistent with the
431 results in Figures 5 and 7, 100% (12/12) of the mice that remained on FLX alone and received
432 Activin A infusions into DG showed decreased latency to eat and were converted into
433 responders ($p < 0.0001$ relative to FLX alone, logrank Mantel-Cox test with Bonferroni
434 correction) (Figure 8b-c). By contrast, only 28.5% (4/14) of the mice switched to sertraline ($p =$
435 0.0408 relative to FLX alone, logrank Mantel-Cox test, not significant with Bonferroni
436 correction), 30.8% (4/13) of the mice switched to bupropion ($p = 0.0329$, logrank Mantel-Cox

bioRxiv preprint doi: https://doi.org/10.1101/491613; this version posted December 10, 2018. The copyright holder for this preprint (which was not certified by peer review) is the author/funder. All rights reserved. No reuse allowed without permission.

437 test, not significant with Bonferroni correction), 35.6% (5/14) of the mice switched to
438 venlafaxine ($p = 0.0193$, logrank Mantel-Cox test, not significant with Bonferroni correction),
439 and 38.5% (5/13) of the mice that remained on FLX and were augmented with bupropion ($p =$
440 0.0145, logrank Mantel-Cox test, not significant with Bonferroni correction) were converted
441 into responders. Therefore, only the chronic DG Activin A infused group showed a
442 significantly decreased latency to eat in NSF relative to the FLX only group. These data
443 strongly suggest that direct modulation of Activin signaling in the DG may be a more effective
444 augmentation strategy than those that are currently used.

bioRxiv preprint doi: https://doi.org/10.1101/491613; this version posted December 10, 2018. The copyright holder for this preprint (which was not certified by peer review) is the author/funder. All rights reserved. No reuse allowed without permission.

445 **DISCUSSION**

446 Our results demonstrate that FLX response status is conserved across several negative
447 valence behavior tests (mice that show a response to FLX in NSF also show a response in EPM
448 and FST and vice versa for non-responders) regardless of whether chronic corticosterone or
449 chronic social defeat stress was used to induce a negative affective state. Furthermore, FLX
450 response status was highly correlated with DG expression of multiple Activin signaling
451 components. Functionally, chronic activation of Activin signaling in the DG successfully
452 converted behavioral non-responders to FLX into responders. By contrast, chronic inhibition of
453 Activin signaling in the DG converted responders to FLX into non-responders. This bidirectional
454 modification is the first evidence that response or resistance to an antidepressant can be altered.
455 Furthermore, these results strongly suggest that Activin signaling in the DG is a necessary
456 component of achieving a behavioral response to antidepressant. Finally, chronic activation of
457 Activin signaling proved to be a more effective augmentation strategy for non-responders to
458 FLX than several commonly used second-line treatments.

459

460 ***Antidepressant Treatment Resistance***

461 Within the United States, approximately 16% of the population will experience an
462 episode of major depression in their lifetime[1]. Although commonly used treatments, such as
463 SSRIs, are prescribed to relieve symptoms, only a subset of patients (~33%) achieve remission
464 with initial treatment[3]. Given that SSRIs are also prescribed widely for several anxiety disorders
465 and obsessive-compulsive disorder, this treatment resistance results in clinicians using decision-
466 tree medical algorithms, such as the Texas Medication Algorithm Project (TMAP)[45], in attempts
467 to combat mood disorders in patients that do not remit to initial lines of treatment. As patients
468 move through different levels of these treatment algorithms, remission rates drop dramatically

bioRxiv preprint doi: https://doi.org/10.1101/491613; this version posted December 10, 2018. The copyright holder for this preprint (which was not certified by peer review) is the author/funder. All rights reserved. No reuse allowed without permission.

469 (~35% with second treatment to ~16% with fourth treatment)[2,46,47]. Therefore, failure to achieve
470 remission within two treatments results in very poor outcomes. These issues plague modern
471 psychiatry and indicate that drugs targeting monoaminergic systems have reached a limit in
472 terms of effectiveness. Much research now focuses on developing drugs that take aim at distinct
473 targets, including glutamate modulators, anticholinergic agents, and opioid modulators rather
474 than monoaminergic systems[48-53]. However, it remains unclear why SSRIs and other
475 monoaminergic drugs are only effective for a subset of patients. Our unique approach here to
476 assess SSRI treatment resistance in mice suggests that individual molecular differences within
477 the neural circuitry underlying the antidepressant response may underlie response status. Direct
478 activation of Activin signaling in the DG proved to be more effective in converting non-
479 responders to FLX treatment into responders. Therefore, similar directed molecular or even
480 neural circuit-based approaches may ultimately prove to be more effective augmentation
481 strategies than blindly switching treatments.
482
483 ***Dentate Gyrus is a critical component of the neural circuitry mediating the antidepressant***
484 ***response***
485 We assessed molecular differences between FLX responders and non-responders in the
486 DG of mice exposed to chronic stress. Our data suggests that manipulation of DG Activin
487 signaling can bidirectionally alter the behavioral response to FLX. These data further support a
488 growing preclinical literature utilizing ablation, genetic, and neural circuit-based approaches to
489 demonstrate that the DG is a principal component of the neural circuitry regulating both mood
490 and the antidepressant treatment response[6,9,11,12,19-22]. It remains to be determined whether neural

bioRxiv preprint doi: https://doi.org/10.1101/491613; this version posted December 10, 2018. The copyright holder for this preprint (which was not certified by peer review) is the author/funder. All rights reserved. No reuse allowed without permission.

491 circuit-based approaches to modify the DG can alter antidepressant response status in a similar
492 fashion to Activin A infusions.
493 Several distinct populations of cells in the DG, including the young adult born granule
494 cells (younger than 8 weeks)[7,9,11], mature granule cells (developmentally born or adult born
495 granule cells older than 8 weeks)[6], and cytocholecystokinin (CCK)-positive GABAergic
496 interneurons[22] are implicated in mediating the antidepressant treatment response. In all
497 likelihood, these distinct populations work in concert via local microcircuitry. One common
498 thread among these cell types is that the young adult born granule cells and CCK-positive
499 interneurons provide an inhibitory influence over the mature granule cells in the ventral DG that
500 is critical for both stress resilience and the antidepressant response[20,22]. Furthermore, inhibitory
501 5-HT1A receptors on mature granule cells are required for the antidepressant response[6]. Our
502 preliminary microarray data that implicated Activin signaling components in the antidepressant
503 response and all data in this manuscript were from microdissections of the granule cell layer
504 (GCL) of the DG[38], which is primarily composed of densely packed mature granule cells and
505 sparse young adult born granule cells[54]. Therefore, we hypothesize that the Activin signaling
506 components are being altered within these cell types. However, it will be important for future
507 work to detail the exact effects of Activin signaling on DG neuronal ensembles, and how Activin
508 signaling affects DG activity and ultimately other components of the neural circuitry underlying
509 the antidepressant response.
510
511 ***The role of Activin signaling in the antidepressant response***
512 The importance of Activin and Inhibin signaling, as part of the TGF-β superfamily, is
513 well-understood in the context of development, where Activin plays important roles in erythroid

bioRxiv preprint doi: https://doi.org/10.1101/491613; this version posted December 10, 2018. The copyright holder for this preprint (which was not certified by peer review) is the author/funder. All rights reserved. No reuse allowed without permission.

514 cell differentiation, induction of the dorsal mesoderm, and craniofacial development[41,55,56].
515 Activin also plays an essential role in pituitary follicle-stimulating hormone (FSH) production,
516 while Inhibin inhibits FSH production[41,55]. However, the roles of these protein complexes are
517 less understood in the context of the developed brain. While basal levels are low, Activin A is
518 rapidly induced in the hippocampus by electroconvulsive seizures and long-term potentiation
519 (LTP)-inducing high frequency stimulation, where it plays a role in the maintenance of long-term
520 memory and late-LTP[57-60]. Activin A and Acvr1A mRNA are upregulated in the DG by chronic
521 treatment with the antidepressant paroxetine and Smad2 phosphorylation is induced by
522 fluoxetine treatment[16,17]. Environmental enrichment (EE) induces Activin A mRNA expression
523 in DG and CA3 and increases Smad2/3 phosphorylation in the hippocampus[60]. Overexpression
524 of a dominant-negative Acvr1B in mouse forebrain under the CamKIIα promoter resulted in
525 anxiolytic-like behavioral effects, a decreased behavioral response to benzodiazepines, enhanced
526 spontaneous GABA release, and increased GABA tonus[61]. Inducible transgenic expression of
527 Activin A under the CamKIIα promoter resulted in anxiolytic-like behavioral effects in the Open
528 Field, EPM, and Light-Dark Test, while expression of Follistatin, an inhibitor of Activin
529 signaling, under the CamKIIα promoter had anxiogenic effects[62]. Furthermore, acute Activin A
530 infusions into DG but not CA1 or Amygdala, reduces immobility in FST[16,17]. Acute Activin B
531 infusions had no effect. Finally, a human genetic association study found 166 single nucleotide
532 polymorphisms (SNPs) within 10 genes belonging to the Activin signaling pathway as being
533 associated with antidepressant treatment response[17]. Genetic variants in the betaglycan gene
534 (*TGFBR3*), a member of the human Activin system, showed the best association, as homozygote
535 carriers of the major allele were significantly more frequent among the responders to

bioRxiv preprint doi: https://doi.org/10.1101/491613; this version posted December 10, 2018. The copyright holder for this preprint (which was not certified by peer review) is the author/funder. All rights reserved. No reuse allowed without permission.

536 antidepressant treatment[17]. Taken together with our results, it is now clear that Activin signaling
537 in the DG is a critical component of the behavioral response to antidepressant treatment.

bioRxiv preprint doi: https://doi.org/10.1101/491613; this version posted December 10, 2018. The copyright holder for this preprint (which was not certified by peer review) is the author/funder. All rights reserved. No reuse allowed without permission.

538 **ACKNOWLEDGEMENTS**

539 This work was supported by: NIMH (R01MH112861 and K01MH098188, B.A.S.) and BBRF
540 NARSAD Young Investigator Award (B.A.S.). The authors thank Dr. Rene Hen for his guidance
541 and mentorship throughout this project, Alice Hu for technical support, and Drs. Dirk Moore and
542 John McGann for their advice on statistical analyses.

543

544 **AUTHOUR CONTRIBUTIONS**

545 B.A.S. conceived experiments. B.A.S., M.R.L., C.N.Y., and M.M.G. performed the experiments.
546 B.A.S., M.M.G., and C.N.Y. analyzed the data and made the figures. C.N.Y., M.M.G., and
547 B.A.S. wrote the manuscript.

548

549 **COMPETING INTERESTS STATEMENT**

550 Authors declare no competing interests.

551

552

bioRxiv preprint doi: https://doi.org/10.1101/491613; this version posted December 10, 2018. The copyright holder for this preprint (which was not certified by peer review) is the author/funder. All rights reserved. No reuse allowed without permission.

553 **METHODS**

554 ***Mice***. Adult 8-week-old male mice purchased from Jackson labs were housed in groups of three
555 to five per cage with *ad libitum* access to food and water. Mice were on a 12:12-h light/dark
556 schedule. All behavioral testing was conducted during the light period and using the same testing
557 time throughout the experiments. Mouse protocols were approved by the Institutional Animal
558 Care and Use Committee at either Columbia University or at Rutgers, The State University of
559 New Jersey.

560

561 ***Drug administration***. Animals were either placed on chronic doses of either vehicle, which
562 consisted of 0.45% β-cyclodextrin in water, or corticosterone (5mg/kg) dissolved in vehicle for
563 duration of experiments. After 4 weeks of either vehicle or corticosterone administration, a
564 subgroup of animals received either vehicle (autoclaved water) or fluoxetine (18mg/kg) via daily
565 oral gavage for throughout the experiment. On the days when mice were subjected to behavioral
566 testing, fluoxetine or vehicle administrations were conducted after the mice completed the testing
567 in order to avoid any acute effects. For additional therapies mice were then treated for 3 weeks
568 with either: bupropion (10mg/kg), venlafaxine (20mg/kg), sertraline (10mg/kg), or fluoxetine +
569 bupropion (18mg/kg, 10mg/kg, respectively) via oral gavage.

570

571 ***Behavioral testing***. Behavioral testing was conducted after 3 weeks of antidepressant
572 administration, in the following order: EPM, NSF and then FST. Mice were given 3 days
573 between behavioral tests to avoid contaminating stressors as well as before sacrifice. Prior to
574 each behavioral test mice were acclimated to the room for 30 mins of habituation.
575 *Elevated plus maze*. EPM was performed as previously described[6]. The plus maze consisted of
576 two closed arms and two open arms 2 feet above the floor. Mice were placed into the central area

bioRxiv preprint doi: https://doi.org/10.1101/491613; this version posted December 10, 2018. The copyright holder for this preprint (which was not certified by peer review) is the author/funder. All rights reserved. No reuse allowed without permission.

577 facing one closed arm and allowed to explore the maze for 5 mins. Data were scored using
578 Ethovision software (Noldus), in which open arm time and open arm entries were recorded.
579 Between animals, the maze was cleaned with 70% ethanol between each run.
580 *Novelty-suppressed feeding*. NSF was performed as described[6,63]. The testing apparatus consisted
581 of a plastic box (50 × 50 × 20 cm), the floor of which was covered with approximately 2 cm of
582 bedding. 18 h before behavioral testing, mice were weighed and food deprived. At the time of
583 testing, a single pellet of food was placed on a white paper platform in the center of the box
584 beneath a gooseneck lamp illuminating the center of the area at about 1500 lux. A mouse was
585 placed in a corner of the box and latency to approach and eat the food pellet was recorded with a
586 maximum of 10 mins. Immediately after the testing period, the mice were transferred to their
587 home cages and latency to feed in the home cage as well as consumption was recorded. After
588 completing testing, animals were weighed again and % change in body weight was calculated
589 with respective to pre-testing weights.
590 *Forced swim test*. As previously described[6], mice were placed into clear plastic buckets 20 cm in
591 diameter and 23 cm deep, filled two-thirds of the way up with 26 °C water and were videotaped.
592 Mice were in the forced swim buckets for 6 mins, but only the last 4 mins were scored. Scoring
593 was automated using Videotrack software (ViewPoint).
594
595 ***Social Defeat Stress***. Paradigm was conducted as previously described. In brief, defeat stress
596 was carried out using similar methods to those already published[20,31]. Prior to social defeat stress,
597 male retired breeder CD1 mice (Charles River Labs) were screened for aggression. CD1 mice
598 that attacked screener mice (C57/BL6J) for two consecutive days in less than 60 seconds were
599 selected. After selection of aggressors, experimental mice were exposed to a different CD1

bioRxiv preprint doi: https://doi.org/10.1101/491613; this version posted December 10, 2018. The copyright holder for this preprint (which was not certified by peer review) is the author/funder. All rights reserved. No reuse allowed without permission.

600 aggressor mouse each day for 5 min over 10 days. After contact, experimental mice were
601 inspected for injury and separated from the aggressor and placed in an adjacent compartment of
602 the same cage as the CD1 mouse, separated by a plastic divider with holes. Control test mice
603 were housed in equivalent cages but with members of the same strain, which were changed daily.
604 Twenty-four hours after the last session, all mice were housed individually for the remainder of
605 the study. Following 10 days of social defeat stress, animals were run through a social interaction
606 test in which mice were placed in an open field for 2.5 minutes for baseline exploration in the
607 absence of a novel CD1, and then for another 2.5 minutes in the presence of a CD1. Mice were
608 deemed susceptible if they spent less time in the interaction zone when the social target was
609 present than absent AND a total time spent interacting with the social target <30s, and resilient if
610 the they spent more time in the interaction zone when the social target was present than absent
611 AND total time spent interacting with the social target >60s.
612
613 ***Gene Expression***. Animals were sacrificed via rapid decapitation and dentate gyrus was
614 microdissected, flash frozen, and then stored at -80°C until further processing. RNA was
615 extracted from tissue samples using a RNA/DNA Purification kit (Norgen Biotek). Total RNA
616 was then converted into cDNA using Superscript III enzyme (Invitrogen). Quantitative-PCR was
617 performed in triplicate reactions with Taqman Fast Advanced Mastermix and Taqman probes for
618 activin a, acvr1a, acvr1b, acvr1c, smad2, smad3, and rn18s (Life Technologies) on a StepOne
619 Plus Real-Time PCR System (Applied Biosystems). Data was analyzed using the $\Delta\Delta C_T$ method,
620 triplicate cycle thresholds per gene per sample were averaged, normalized to control gene
621 (*rn18s*) to obtain ΔC_T, and were then converted to $\Delta\Delta C_T$ values by normalizing to mean ΔC_T's of

bioRxiv preprint doi: https://doi.org/10.1101/491613; this version posted December 10, 2018. The copyright holder for this preprint (which was not certified by peer review) is the author/funder. All rights reserved. No reuse allowed without permission.

622 the vehicle group. Final values were then expressed as an expression percentage relative to the
623 vehicle group values.
624
625 ***Intracerebral infusions***. Mice were anesthetized with sodium pentobarbital (diluted 1:10 from
626 stock of 50mg/ml and injected at a volume of 10 ml/kg) and guide cannulae with dummy
627 cannulae (Plastics 1) were implanted. For ventral DG the coordinates used were: -3.5 mm and
628 ±2.8 mm from bregma at a depth of 3.6mm from the skull surface, and for CA1 the coordinates
629 used were: -3.1mm and ±3.0mm from the bregma at a depth of 2.0mm from the skull surface. 1-
630 2 weeks after surgery, animals began to receive bilateral infusions of either vehicle (0.1% BSA),
631 1μg of mouse Activin A peptide (R&D Systems), 1μg of mouse Inhibin A peptide (R&D
632 Systems), or 1μg each of Activin A+Inhibin A in vehicle once per day (over a time course of 15
633 minutes per side, 10 minutes of infusion and an additional 5 minutes with tubing left in place) for
634 2 weeks prior to behavioral testing. Each day connector assemblies with tubing were connected
635 to internal cannulae, which were then inserted into the guide cannulae. Infusions were delivered
636 by a standard infusion only syringe pump (Harvard Apparatus). A total volume of 1.0 μl was
637 infused in each hemisphere per day. Animals were freely moving in their cage during infusions.
638
639 ***Statistics***. All statistics were performed using Prism Software 7 (Graphpad). Parametric
640 hypotheses were assessed with parametric tests. Two-way ANOVAs assessing stress
641 pretreatment x antidepressant treatment were used for EPM, FST, Negative Affect Index, and
642 gene expression. One-way ANOVAs were then subsequently used to assess Stress+VEH,
643 Stress+FLX responders, and Stress+FLX non-responders. NSF was assessed using non-
644 parametric Kaplan Meier survival analysis with log-rank Mantel-Cox. Correlational analysis

bioRxiv preprint doi: https://doi.org/10.1101/491613; this version posted December 10, 2018. The copyright holder for this preprint (which was not certified by peer review) is the author/funder. All rights reserved. No reuse allowed without permission.

645 between individual animal behavioral values (NSF and either EPM or FST) were performed
646 using Pearson r and best-fit values with a linear regression analysis and slopes with analysis
647 significant non-zeroes were analyzed. Post hoc Bonferroni corrections were used where
648 appropriate.

bioRxiv preprint doi: https://doi.org/10.1101/491613; this version posted December 10, 2018. The copyright holder for this preprint (which was not certified by peer review) is the author/funder. All rights reserved. No reuse allowed without permission.

649 **FIGURE LEGENDS**

650 **Figure 1** *Behavioral Responders and Non-Responders to FLX treatment following CORT*
651 *administration* (a) Timeline of experiment. (b) Kaplan-Meier survival curve (large panel) and
652 scatterplot (small panel) of NSF data showing individual latency to eat values across all four
653 treatment groups. (c-e) Two-way ANOVA of all treatment groups (small panel) and One-Way
654 ANOVA of CORT+VEH, CORT+FLX responders and CORT+FLX non-responders (large
655 panel) for EPM open arm entries (c left panel), EPM open arm duration (c right panel), FST
656 immobility (d), and Negative Affect Index (e). (f) Regression analyses correlating NSF latency
657 to eat with FST immobility (left) and EPM open arm duration (right). (g) In a separate cohort of
658 CORT+FLX mice, persistence of response was determined by assessing NSF behavior after 3
659 weeks of FLX (time point 0), and then again 1, 4, and 6 months later. For survival curves, line
660 shading shows SEM of each group (n=15-23 per group). Scatterplots, horizontal lines, and bars
661 show group means with errors bars indicating SEM (n=7-16 per group).

662

663 **Figure 2** *Dentate Gyrus mRNA expression of Activin signaling components correlates with*
664 *behavioral response to FLX treatment following CORT administration* (a-f) Two-Way ANOVA
665 of all treatment groups (middle panels), One-Way ANOVA of CORT+VEH, CORT+FLX
666 responders and CORT+FLX non-responders (left panels), and regression analyses correlating
667 NSF latency to eat with DG mRNA expression of activin A (a), acvr1a (b), acvr1b (c), acvr1c
668 (d), smad2 (e), and smad3 (f). Scatterplots, horizontal lines, and bars show group means with
669 errors bars indicating SEM (n=12-14 per group).

670

bioRxiv preprint doi: https://doi.org/10.1101/491613; this version posted December 10, 2018. The copyright holder for this preprint (which was not certified by peer review) is the author/funder. All rights reserved. No reuse allowed without permission.

671 **Figure 3** *Behavioral Responders and Non-Responders to FLX treatment following* CSDS (a)
672 Timeline of experiment and diagram of CSDS and Social Interaction (SIT) protocol. (b) Kaplan-
673 Meier survival curve (large panel) and scatterplot (small panel) of NSF data showing individual
674 latency to eat values across all four treatment groups. (c-e) Two-way ANOVA of all treatment
675 groups (small panel) and One-Way ANOVA of SUS+VEH, SUS+FLX responders and
676 SUS+FLX non-responders (large panel) for EPM open arm entries (c left panel), EPM open arm
677 duration (c right panel), FST immobility (d), and Negative Affect Index (e). (f) Regression
678 analyses correlating NSF latency to eat with FST immobility (left) and EPM open arm duration
679 (right). For survival curves, line shading shows SEM of each group (n=12-14 per group).
680 Scatterplots, horizontal lines, and bars show group means with errors bars indicating SEM (n=6-
681 18 per group).
682
683 **Figure 4** *Dentate Gyrus mRNA expression of Activin signaling components correlates with*
684 *behavioral response to FLX treatment following CSDS administration* (a-f) Two-Way ANOVA
685 of all treatment groups (middle panels), One-Way ANOVA of CORT+VEH, CORT+FLX
686 responders and CORT+FLX non-responders (left panels), and regression analyses correlating
687 NSF latency to eat with DG mRNA expression of activin A (a), acvr1a (b), acvr1b (c), acvr1c
688 (d), smad2 (e), and smad3 (f). Scatterplots, horizontal lines, and bars show group means with
689 errors bars indicating SEM (n=6-12 per group).
690
691 **Figure 5** *Chronic Activin A infusions into DG convert FLX non-responders into responders* (a)
692 Timeline of experiment and coordinates of infusions for ventral DG and ventral CA1. (b)
693 Kaplan-Meier survival curve (large panel) and scatterplot (small panel) of NSF data showing

bioRxiv preprint doi: https://doi.org/10.1101/491613; this version posted December 10, 2018. The copyright holder for this preprint (which was not certified by peer review) is the author/funder. All rights reserved. No reuse allowed without permission.

694 individual latency to eat values across all three non-responder treatment groups. (c-e) One-Way
695 ANOVA of VEH, Activin A infusions into DG ($ACTIVIN_{DG}$), and Activin A infusions into CA1
696 ($ACTIVIN_{CA1}$) for EPM open arm entries (c left panel), EPM open arm duration (c right panel),
697 FST immobility (d), and Negative Affect Index (e). (f) Regression analyses correlating NSF
698 latency to eat with EPM open arm duration (left) and FST immobility (right). For survival
699 curves, line shading shows SEM of each group (n=12 per group). Scatterplots, horizontal lines,
700 and bars show group means with errors bars indicating SEM.
701
702 **Figure 6** *Inhibition of Activin signaling in DG converts FLX responders into non-responders* (a)
703 Timeline of experiment and coordinates of infusions for ventral DG and ventral CA1. (b)
704 Kaplan-Meier survival curve (large panel) and scatterplot (small panel) of NSF data showing
705 individual latency to eat values across all three responder treatment groups. (c-e) One-Way
706 ANOVA of VEH, Inhibin A infusions into DG ($INHIBIN_{DG}$), and Inhibin A infusions into CA1
707 ($INHIBIN_{CA1}$) for EPM open arm entries (c left panel), EPM open arm duration (c right panel),
708 FST immobility (d), and Negative Affect Index (e). (f) Regression analyses correlating NSF
709 latency to eat with EPM open arm duration (left) and FST immobility (right). For survival
710 curves, line shading shows SEM of each group (n=12 per group). Scatterplots, horizontal lines,
711 and bars show group means with errors bars indicating SEM.
712
713 **Figure 7** *Coinfusion of Activin A and Inhibin A into Non-Responders blocks the effects of Activin*
714 *A on behavior* (a) Timeline of experiment and coordinates of infusions for ventral DG. (b)
715 Kaplan-Meier survival curve (large panel) and scatterplot (small panel) of NSF data showing
716 individual latency to eat values across all four non-responder treatment groups. (c-e) One-Way

bioRxiv preprint doi: https://doi.org/10.1101/491613; this version posted December 10, 2018. The copyright holder for this preprint (which was not certified by peer review) is the author/funder. All rights reserved. No reuse allowed without permission.

717 ANOVA of VEH, Activin A infusions into DG (ACTIVIN$_{DG}$), Inhibin A infusions into DG
718 (INHIBIN$_{DG}$), and combined Activin A and Inhibin A infusions into DG
719 (ACTIVIN+INHIBIN$_{DG}$) for EPM open arm entries (c left panel), EPM open arm duration (c
720 right panel), FST immobility (d), and Negative Affect Index (e). (f) Regression analyses
721 correlating NSF latency to eat with EPM open arm duration (left) and FST immobility (right).
722 For survival curves, line shading shows SEM of each group (n=12 per group). Scatterplots,
723 horizontal lines, and bars show group means with errors bars indicating SEM.
724
725 **Figure 8** ***Activin A infusions into DG are a more effective augmentation therapy than***
726 ***commonly used second-line treatments*** (a) Timeline of experiment. (b) Kaplan-Meier survival
727 curve (large panel) and scatterplot (small panel) of NSF data showing individual latency to eat
728 values across all six CORT+FLX non-responder treatment groups. (c) Graphical depiction of
729 proportion of CORT+FLX non-responders converted into responders following the different
730 second-line treatments.
731
732 **Supplemental Figure 1**. *NSF data for DG mRNA expression cohort of mice and serum FLX*
733 *levels* (a) Timeline of experiment. (b) Kaplan-Meier survival curve (large panel) and scatterplot
734 (small panel) of NSF data showing individual latency to eat values across all four treatment
735 groups. (c) Two-way ANOVA of all treatment groups (small panel) and One-Way ANOVA of
736 CORT+VEH, CORT+FLX responders and CORT+FLX non-responders (large panel) for serum
737 FLX levels following three weeks of FLX administration. For survival curves, line shading
738 shows SEM of each group (n=15-23 per group). Scatterplots, horizontal lines, and bars show
739 group means with errors bars indicating SEM.

bioRxiv preprint doi: https://doi.org/10.1101/491613; this version posted December 10, 2018. The copyright holder for this preprint (which was not certified by peer review) is the author/funder. All rights reserved. No reuse allowed without permission.

740

741 **Supplemental Figure 2**. *Identification and classification of susceptible mice in Figures 3 and 4*

742 (a) Timeline of experiment and diagram of CSDS and Social Interaction (SIT) protocol. (b) Time

743 spent in social interaction zone reveal significant difference ($F_{(3,67)} = 106$, $p < 0.0001$) only in the

744 presence of a CD1 aggressor. The only difference between groups was CNTRL animals

745 compared to SUS+VEH ($p < 0.0001$, Bonferroni-corrected), SUS+FLX-R ($p < 0.0001$,

746 Bonferroni-corrected), or SUS+FLX-NR ($p < 0.0001$, Bonferroni-corrected). (b) Social

747 interaction ratios were significantly different ($F_{(4,66)} = 62.2$, $p < 0.0001$). The only difference

748 between groups was CNTRL animals compared to SUS+VEH ($p < 0.0001$, Bonferroni-

749 corrected), SUS+FLX-R ($p < 0.0001$, Bonferroni-corrected), and SUS+FLX-NR ($p < 0.0001$,

750 Bonferroni-corrected).

751

752

bioRxiv preprint doi: https://doi.org/10.1101/491613; this version posted December 10, 2018. The copyright holder for this preprint (which was not certified by peer review) is the author/funder. All rights reserved. No reuse allowed without permission.

753 **REFERENCES**

754 1 Kessler, R. C. *et al.* The epidemiology of major depressive disorder: results from the
755 National Comorbidity Survey Replication (NCS-R). *JAMA* **289**, 3095-3105,
756 doi:10.1001/jama.289.23.3095 (2003).
757 2 Warden, D., Rush, A. J., Trivedi, M. H., Fava, M. & Wisniewski, S. R. The STAR*D
758 Project results: a comprehensive review of findings. *Curr Psychiatry Rep* **9**, 449-459
759 (2007).
760 3 Trivedi, M. H. *et al.* Evaluation of outcomes with citalopram for depression using
761 measurement-based care in STAR*D: implications for clinical practice. *The American*
762 *journal of psychiatry* **163**, 28-40, doi:10.1176/appi.ajp.163.1.28 (2006).
763 4 Drevets, W. C. Neuroimaging and neuropathological studies of depression: implications
764 for the cognitive-emotional features of mood disorders. *Curr Opin Neurobiol* **11**, 240-249
765 (2001).
766 5 Nestler, E. J. *et al.* Neurobiology of depression. *Neuron* **34**, 13-25 (2002).
767 6 Samuels, B. A. *et al.* 5-HT1A receptors on mature dentate gyrus granule cells are critical
768 for the antidepressant response. *Nature Neuroscience* **18**, 1606-1616,
769 doi:10.1038/nn.4116 (2015).
770 7 Malberg, J. E., Eisch, A. J., Nestler, E. J. & Duman, R. S. Chronic antidepressant
771 treatment increases neurogenesis in adult rat hippocampus. *J Neurosci* **20**, 9104-9110
772 (2000).
773 8 Wang, J.-W., David, D. J., Monckton, J. E., Battaglia, F. & Hen, R. Chronic fluoxetine
774 stimulates maturation and synaptic plasticity of adult-born hippocampal granule cells. *J*
775 *Neurosci* **28**, 1374-1384, doi:10.1523/JNEUROSCI.3632-07.2008 (2008).
776 9 Santarelli, L. *et al.* Requirement of hippocampal neurogenesis for the behavioral effects
777 of antidepressants. *Science* **301**, 805-809, doi:10.1126/science.1083328 (2003).
778 10 Li, Y. *et al.* TrkB regulates hippocampal neurogenesis and governs sensitivity to
779 antidepressive treatment. *Neuron* **59**, 399-412, doi:10.1016/j.neuron.2008.06.023 (2008).
780 11 David, D. J. *et al.* Neurogenesis-dependent and -independent effects of fluoxetine in an
781 animal model of anxiety/depression. *Neuron* **62**, 479-493,
782 doi:10.1016/j.neuron.2009.04.017 (2009).
783 12 Airan, R. D. *et al.* High-speed imaging reveals neurophysiological links to behavior in an
784 animal model of depression. *Science* **317**, 819-823, doi:10.1126/science.1144400 (2007).
785 13 Shirayama, Y., Chen, A. C., Nakagawa, S., Russell, D. S. & Duman, R. S. Brain-derived
786 neurotrophic factor produces antidepressant effects in behavioral models of depression. *J*
787 *Neurosci* **22**, 3251-3261, doi:20026292 (2002).
788 14 Warner-Schmidt, J. L. & Duman, R. S. VEGF is an essential mediator of the neurogenic
789 and behavioral actions of antidepressants. *Proc Natl Acad Sci USA* **104**, 4647-4652,
790 doi:10.1073/pnas.0610282104 (2007).
791 15 Warner-Schmidt, J. L. & Duman, R. S. VEGF as a potential target for therapeutic
792 intervention in depression. *Current Opinion in Pharmacology* **8**, 14-19,
793 doi:10.1016/j.coph.2007.10.013 (2008).
794 16 Dow, A. L., Russell, D. S. & Duman, R. S. Regulation of activin mRNA and Smad2
795 phosphorylation by antidepressant treatment in the rat brain: effects in behavioral models.
796 *J Neurosci* **25**, 4908-4916, doi:10.1523/JNEUROSCI.5155-04.2005 (2005).

bioRxiv preprint doi: https://doi.org/10.1101/491613; this version posted December 10, 2018. The copyright holder for this preprint (which was not certified by peer review) is the author/funder. All rights reserved. No reuse allowed without permission.

797 17 Ganea, K. *et al.* Convergent animal and human evidence suggests the activin/inhibin
798 pathway to be involved in antidepressant response. *Transl Psychiatry* **2**, e177,
799 doi:10.1038/tp.2012.104 (2012).
800 18 Yun, S. *et al.* Stimulation of entorhinal cortex-dentate gyrus circuitry is antidepressive.
801 *Nat Med* **24**, 658-666, doi:10.1038/s41591-018-0002-1 (2018).
802 19 Kheirbek, M. A. *et al.* Differential Control of Learning and Anxiety along the
803 Dorsoventral Axis of the Dentate Gyrus. *Neuron* **77**, 955-968,
804 doi:10.1016/j.neuron.2012.12.038 (2013).
805 20 Anacker, C. *et al.* Hippocampal neurogenesis confers stress resilience by inhibiting the
806 ventral dentate gyrus. *Nature* **559**, 98-102, doi:10.1038/s41586-018-0262-4 (2018).
807 21 Bagot, R. C. *et al.* Ventral hippocampal afferents to the nucleus accumbens regulate
808 susceptibility to depression. *Nat Commun* **6**, 7062, doi:10.1038/ncomms8062 (2015).
809 22 Medrihan, L. *et al.* Initiation of Behavioral Response to Antidepressants by
810 Cholecystokinin Neurons of the Dentate Gyrus. *Neuron* **95**, 564-576 e564,
811 doi:10.1016/j.neuron.2017.06.044 (2017).
812 23 Boldrini, M. *et al.* Hippocampal granule neuron number and dentate gyrus volume in
813 antidepressant-treated and untreated major depression. *Neuropsychopharmacology* **38**,
814 1068-1077, doi:10.1038/npp.2013.5 (2013).
815 24 Treadway, M. T. *et al.* Illness progression, recent stress, and morphometry of
816 hippocampal subfields and medial prefrontal cortex in major depression. *Biol Psychiatry*
817 **77**, 285-294, doi:10.1016/j.biopsych.2014.06.018 (2015).
818 25 Katz, R. J. Animal model of depression: pharmacological sensitivity of a hedonic deficit.
819 *Pharmacol Biochem Behav* **16**, 965-968 (1982).
820 26 Willner, P. Chronic mild stress (CMS) revisited: consistency and behavioural-
821 neurobiological concordance in the effects of CMS. *Neuropsychobiology* **52**, 90-110,
822 doi:10.1159/000087097 (2005).
823 27 Willner, P., Towell, A., Sampson, D., Sophokleous, S. & Muscat, R. Reduction of
824 sucrose preference by chronic unpredictable mild stress, and its restoration by a tricyclic
825 antidepressant. *Psychopharmacology (Berl)* **93**, 358-364 (1987).
826 28 Surget, A. *et al.* Drug-dependent requirement of hippocampal neurogenesis in a model of
827 depression and of antidepressant reversal. *Biological Psychiatry* **64**, 293-301,
828 doi:10.1016/j.biopsych.2008.02.022 (2008).
829 29 Samuels, B. A. *et al.* Modeling treatment-resistant depression. *Neuropharmacology* **61**,
830 408-413, doi:10.1016/j.neuropharm.2011.02.017 (2011).
831 30 Berton, O. *et al.* Essential role of BDNF in the mesolimbic dopamine pathway in social
832 defeat stress. *Science* **311**, 864-868, doi:10.1126/science.1120972 (2006).
833 31 Tsankova, N. M. *et al.* Sustained hippocampal chromatin regulation in a mouse model of
834 depression and antidepressant action. *Nat Neurosci* **9**, 519-525, doi:10.1038/nn1659
835 (2006).
836 32 Krishnan, V. & Nestler, E. J. The molecular neurobiology of depression. *Nature* **455**,
837 894-902, doi:10.1038/nature07455 (2008).
838 33 Ardayfio, P. & Kim, K.-S. Anxiogenic-like effect of chronic corticosterone in the light-
839 dark emergence task in mice. *Behav Neurosci* **120**, 249-256, doi:10.1037/0735-
840 7044.120.2.249 (2006).

bioRxiv preprint doi: https://doi.org/10.1101/491613; this version posted December 10, 2018. The copyright holder for this preprint (which was not certified by peer review) is the author/funder. All rights reserved. No reuse allowed without permission.

841 34 Gourley, S. L. *et al.* Regionally specific regulation of ERK MAP kinase in a model of
842 antidepressant-sensitive chronic depression. *Biological Psychiatry* **63**, 353-359,
843 doi:10.1016/j.biopsych.2007.07.016 (2008).
844 35 Gourley, S. L., Wu, F. J. & Taylor, J. R. Corticosterone regulates pERK1/2 map kinase in
845 a chronic depression model. *Ann N Y Acad Sci* **1148**, 509-514,
846 doi:10.1196/annals.1410.076 (2008).
847 36 Murray, F., Smith, D. W. & Hutson, P. H. Chronic low dose corticosterone exposure
848 decreased hippocampal cell proliferation, volume and induced anxiety and depression
849 like behaviours in mice. *Eur J Pharmacol* **583**, 115-127,
850 doi:10.1016/j.ejphar.2008.01.014 (2008).
851 37 Slattery, D. A. & Cryan, J. F. Modelling depression in animals: at the interface of reward
852 and stress pathways. *Psychopharmacology (Berl)* **234**, 1451-1465, doi:10.1007/s00213-
853 017-4552-6 (2017).
854 38 Samuels, B. A. *et al.* Global state measures of the dentate gyrus gene expression system
855 predict antidepressant-sensitive behaviors. *PLoS One* **9**, e85136,
856 doi:10.1371/journal.pone.0085136 (2014).
857 39 Guilloux, J. P., Seney, M., Edgar, N. & Sibille, E. Integrated behavioral z-scoring
858 increases the sensitivity and reliability of behavioral phenotyping in mice: relevance to
859 emotionality and sex. *J Neurosci Methods* **197**, 21-31,
860 doi:10.1016/j.jneumeth.2011.01.019 (2011).
861 40 Mekiri, M., Gardier, A. M., David, D. J. & Guilloux, J. P. Chronic corticosterone
862 administration effects on behavioral emotionality in female c57bl6 mice. *Exp Clin*
863 *Psychopharmacol* **25**, 94-104, doi:10.1037/pha0000112 (2017).
864 41 Massagué, J. TGF-beta signal transduction. *Annu Rev Biochem* **67**, 753-791,
865 doi:10.1146/annurev.biochem.67.1.753 (1998).
866 42 Maj, J. & Moryl, E. Effects of sertraline and citalopram given repeatedly on the
867 responsiveness of 5-HT receptor subpopulations. *J Neural Transm Gen Sect* **88**, 143-156
868 (1992).
869 43 Kale, P. P. & Addepalli, V. Augmentation of antidepressant effects of duloxetine and
870 bupropion by caffeine in mice. *Pharmacol Biochem Behav* **124**, 238-244,
871 doi:10.1016/j.pbb.2014.06.005 (2014).
872 44 Berrocoso, E. & Mico, J. A. Role of serotonin 5-HT1A receptors in the antidepressant-
873 like effect and the antinociceptive effect of venlafaxine in mice. *Int J*
874 *Neuropsychopharmacol* **12**, 61-71, doi:10.1017/S1461145708008766 (2009).
875 45 Gilbert, D. A. *et al.* Texas Medication Algorithm Project: definitions, rationale, and
876 methods to develop medication algorithms. *J Clin Psychiatry* **59**, 345-351 (1998).
877 46 Rush, A. J. *et al.* Acute and longer-term outcomes in depressed outpatients requiring one
878 or several treatment steps: a STAR*D report. *Am J Psychiatry* **163**, 1905-1917,
879 doi:10.1176/appi.ajp.163.11.1905 (2006).
880 47 Rush, A. J. *et al.* STAR*D: revising conventional wisdom. *CNS drugs* **23**, 627-647,
881 doi:10.2165/00023210-200923080-00001 (2009).
882 48 Berman, R. M. *et al.* Antidepressant effects of ketamine in depressed patients. *Biological*
883 *Psychiatry* **47**, 351-354 (2000).
884 49 Zarate, C. A. *et al.* A randomized trial of an N-methyl-D-aspartate antagonist in
885 treatment-resistant major depression. *Arch Gen Psychiatry* **63**, 856-864,
886 doi:10.1001/archpsyc.63.8.856 (2006).

bioRxiv preprint doi: https://doi.org/10.1101/491613; this version posted December 10, 2018. The copyright holder for this preprint (which was not certified by peer review) is the author/funder. All rights reserved. No reuse allowed without permission.

887 50 Sanacora, G. *et al.* Lanicemine: a low-trapping NMDA channel blocker produces
888 sustained antidepressant efficacy with minimal psychotomimetic adverse effects. *Mol*
889 *Psychiatry* **19**, 978-985, doi:10.1038/mp.2013.130 (2014).
890 51 Furey, M. L. & Drevets, W. C. Antidepressant efficacy of the antimuscarinic drug
891 scopolamine: a randomized, placebo-controlled clinical trial. *Arch Gen Psychiatry* **63**,
892 1121-1129, doi:10.1001/archpsyc.63.10.1121 (2006).
893 52 Carlezon, W. A., Jr., Beguin, C., Knoll, A. T. & Cohen, B. M. Kappa-opioid ligands in
894 the study and treatment of mood disorders. *Pharmacol Ther* **123**, 334-343,
895 doi:10.1016/j.pharmthera.2009.05.008 (2009).
896 53 Samuels, B. A. *et al.* The Behavioral Effects of the Antidepressant Tianeptine Require
897 the Mu-Opioid Receptor. *Neuropsychopharmacology* **42**, 2052-2063,
898 doi:10.1038/npp.2017.60 (2017).
899 54 Amaral, D. G., Scharfman, H. E. & Lavenex, P. The dentate gyrus: fundamental
900 neuroanatomical organization (dentate gyrus for dummies). *Prog Brain Res* **163**, 3-22,
901 doi:10.1016/S0079-6123(07)63001-5 (2007).
902 55 Pauklin, S. & Vallier, L. Activin/Nodal signalling in stem cells. *Development* **142**, 607-
903 619, doi:10.1242/dev.091769 (2015).
904 56 Ageta, H. & Tsuchida, K. Multifunctional roles of activins in the brain. *Vitam Horm* **85**,
905 185-206, doi:10.1016/B978-0-12-385961-7.00009-3 (2011).
906 57 Andreasson, K. & Worley, P. F. Induction of beta-A activin expression by synaptic
907 activity and during neocortical development. *Neuroscience* **69**, 781-796 (1995).
908 58 Ageta, H. *et al.* Activin plays a key role in the maintenance of long-term memory and
909 late-LTP. *Learn Mem* **17**, 176-185, doi:10.1101/lm.16659010 (2010).
910 59 Link, A. S., Zheng, F. & Alzheimer, C. Activin Signaling in the Pathogenesis and
911 Therapy of Neuropsychiatric Diseases. *Front Mol Neurosci* **9**, 32,
912 doi:10.3389/fnmol.2016.00032 (2016).
913 60 Link, A. S. *et al.* Kdm6b and Pmepa1 as Targets of Bioelectrically and Behaviorally
914 Induced Activin A Signaling. *Mol Neurobiol* **53**, 4210-4225, doi:10.1007/s12035-015-
915 9363-3 (2016).
916 61 Zheng, F. *et al.* Activin tunes GABAergic neurotransmission and modulates anxiety-like
917 behavior. *Mol Psychiatry* **14**, 332-346, doi:10.1038/sj.mp.4002131 (2009).
918 62 Ageta, H. *et al.* Activin in the brain modulates anxiety-related behavior and adult
919 neurogenesis. *PLoS ONE* **3**, e1869, doi:10.1371/journal.pone.0001869 (2008).
920 63 Samuels, B. A. & Hen, R. in *Mood and Anxiety Related Phenotypes in Mice:*
921 *Characterization Using Behavioral Tests, Volume II Neuromethods* (ed Todd D Gould)
922 Ch. 7, 107-121 (Humana Press, 2011).
923

bioRxiv preprint doi: https://doi.org/10.1101/491613; this version posted December 10, 2018. The copyright holder for this preprint (which was not certified by peer review) is the author/funder. All rights reserved. No reuse allowed without permission.

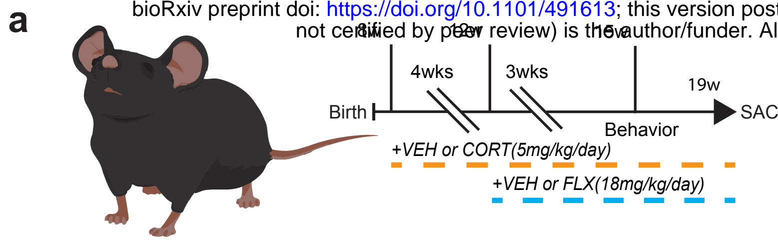

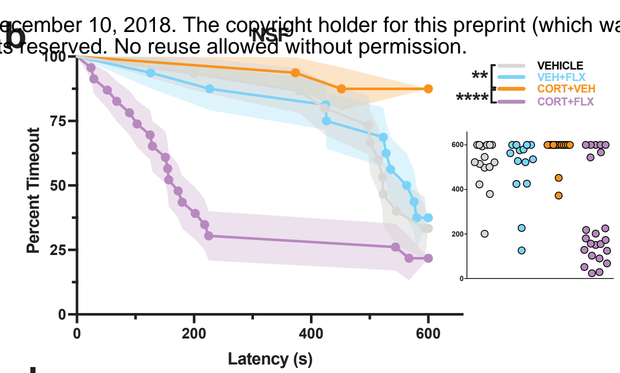

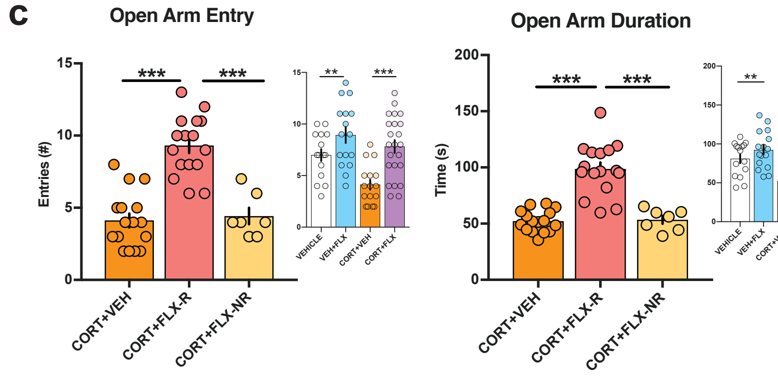

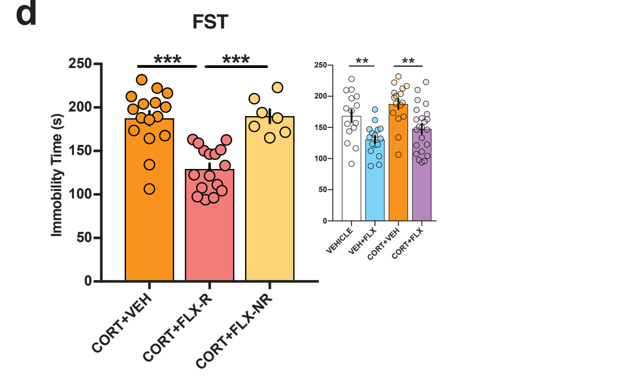

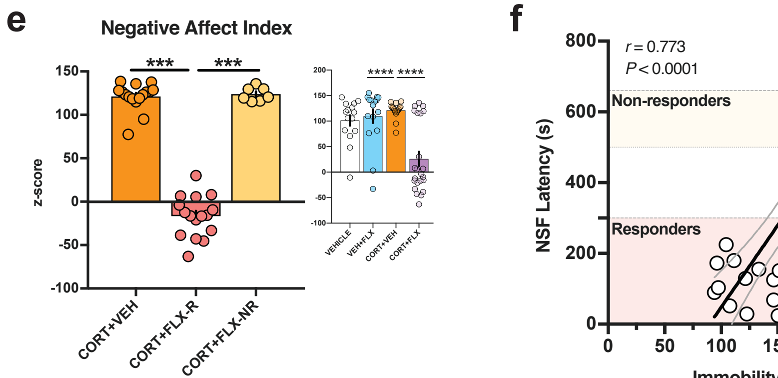

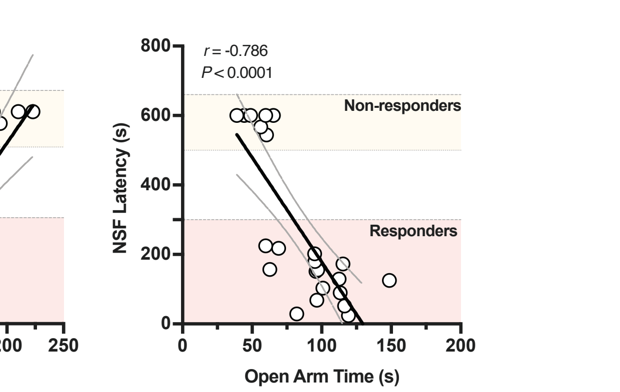

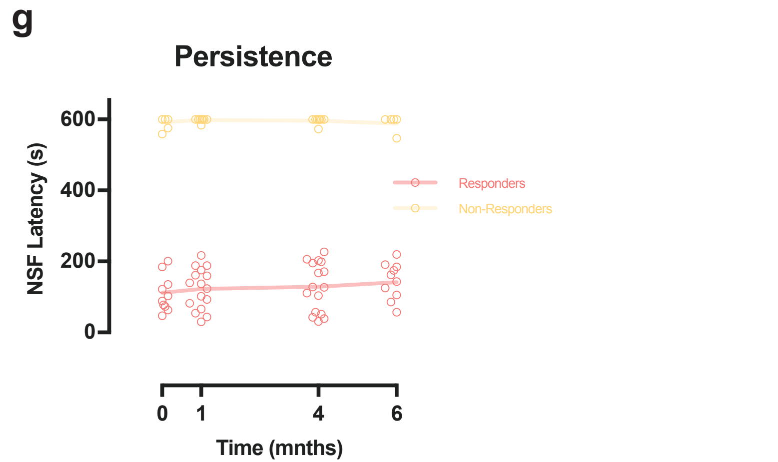

bioRxiv preprint doi: https://doi.org/10.1101/491613; this version posted December 10, 2018. The copyright holder for this preprint (which was not certified by peer review) is the author/funder. All rights reserved. No reuse allowed without permission.

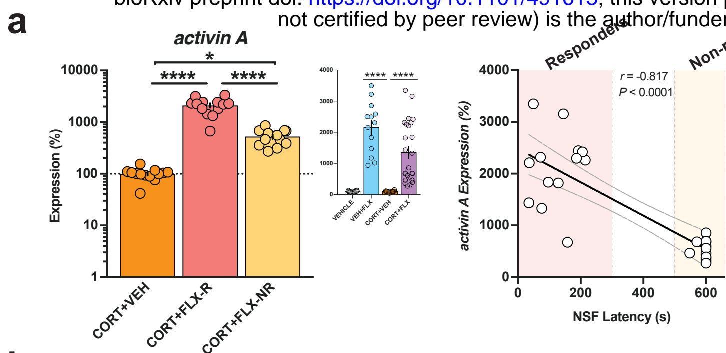

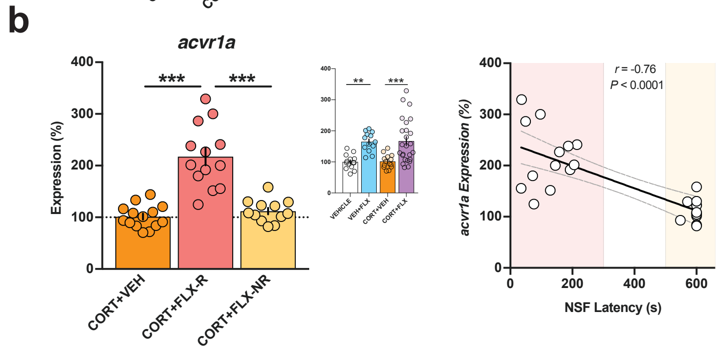

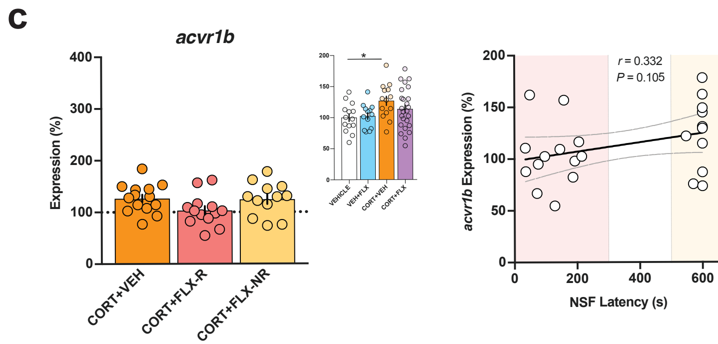

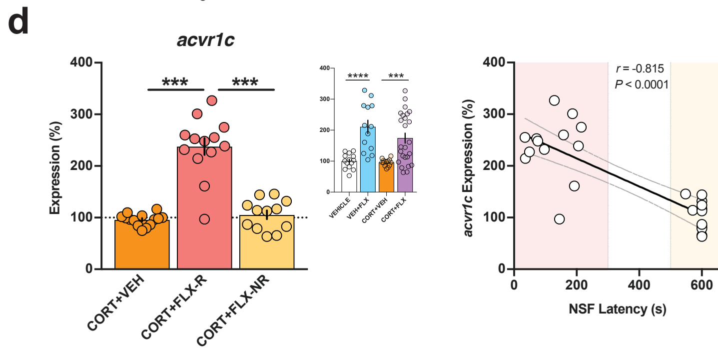

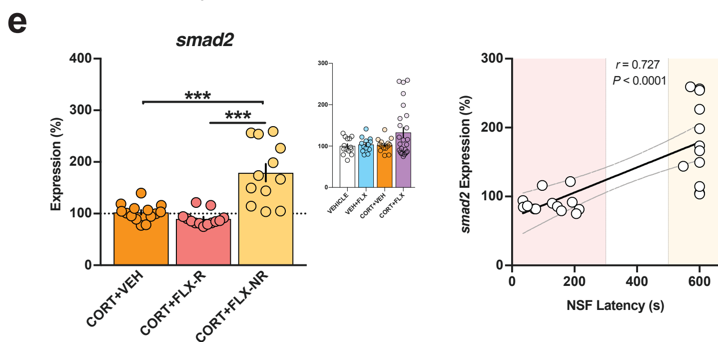

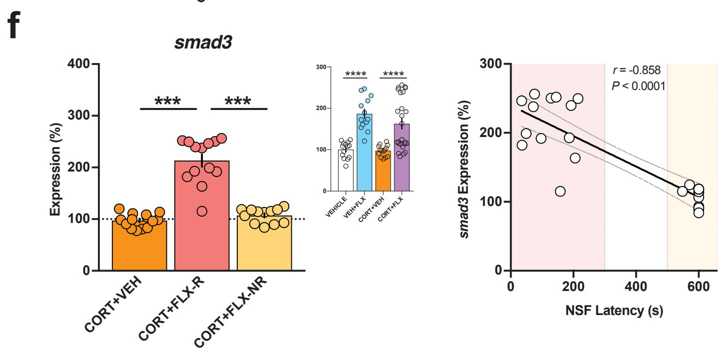

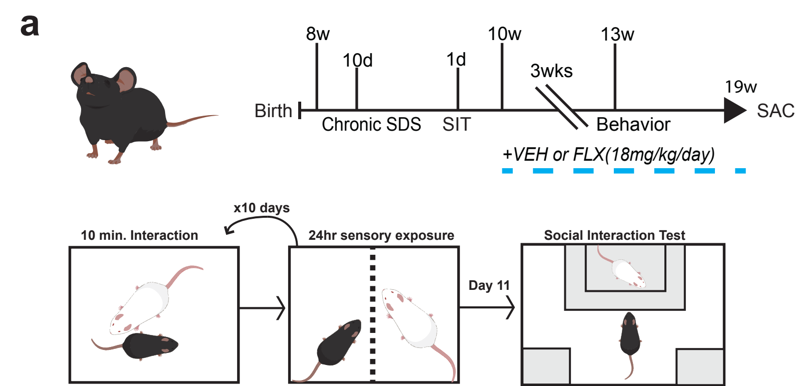
a
8w
10d
1d
10w
3wks
13w
19w
Birth
Chronic SDS
SIT
Behavior
SAC
+VEH or FLX(18mg/kg/day)
x10 days
10 min. Interaction
24hr sensory exposure
Day 11
Social Interaction Test

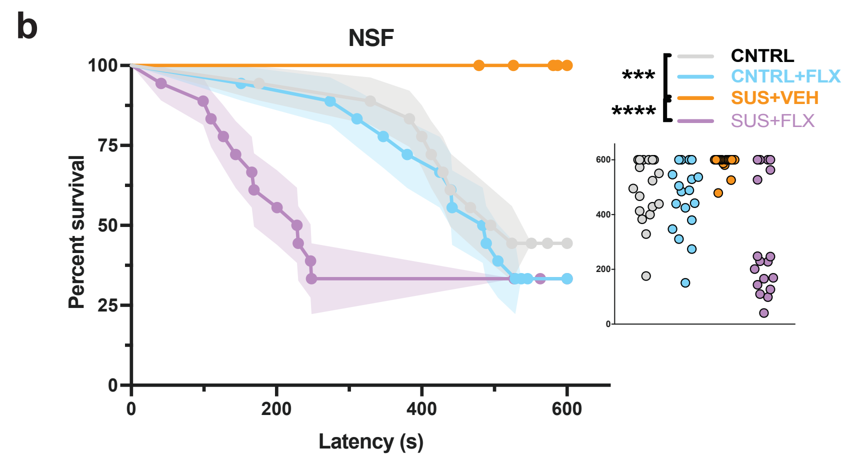
b
NSF
Percent survival
100
75
50
25
0
0
200
400
600
Latency (s)
***
****
CNTRL
CNTRL+FLX
SUS+VEH
SUS+FLX

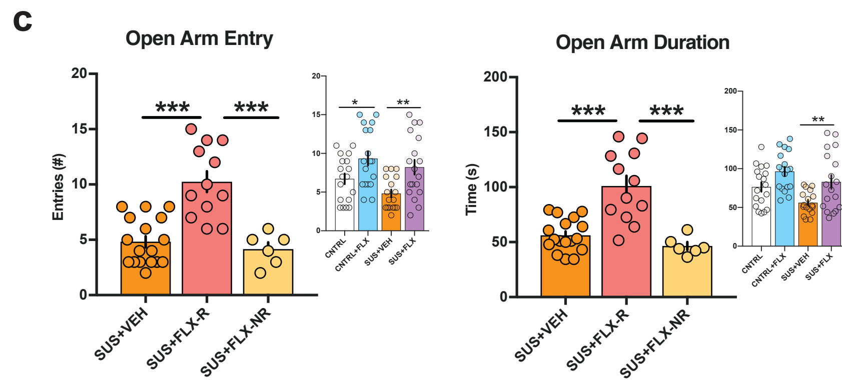
c
Open Arm Entry
Entries (#)
20
15
10
5
0
***
***
SUS+VEH
SUS+FLX-R
SUS+FLX-NR
Open Arm Duration
Time (s)
200
150
100
50
0
***
***
SUS+VEH
SUS+FLX-R
SUS+FLX-NR

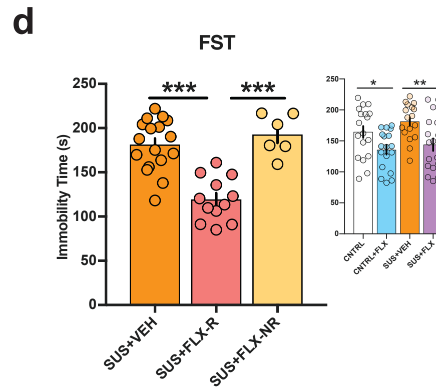
d
FST
Immobility Time (s)
250
200
150
100
50
0
***
***
SUS+VEH
SUS+FLX-R
SUS+FLX-NR

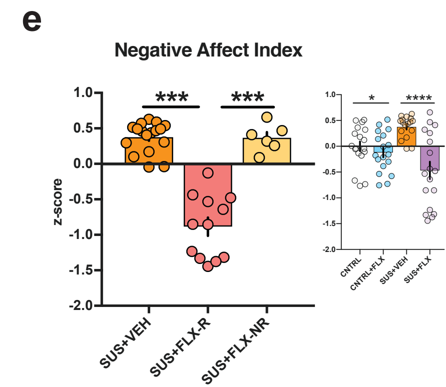
e
Negative Affect Index
z-score
1.0
0.5
0.0
-0.5
-1.0
-1.5
-2.0
***
***
SUS+VEH
SUS+FLX-R
SUS+FLX-NR

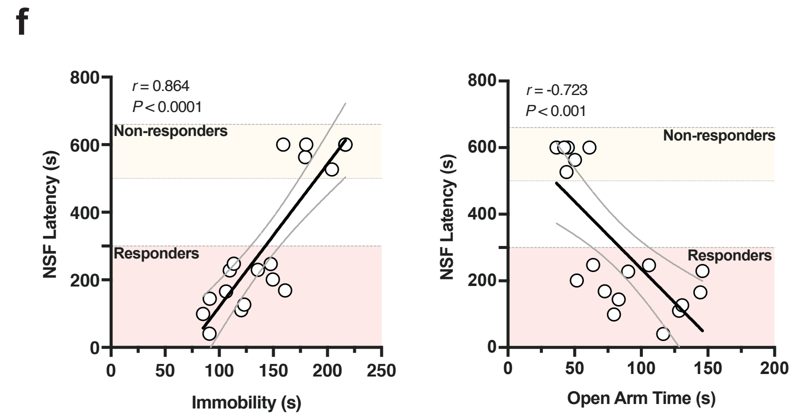
f
r = 0.864
P < 0.0001
Non-responders
Responders
NSF Latency (s)
800
600
400
200
0
0
50
100
150
200
250
Immobility (s)
r = -0.723
P < 0.001
Non-responders
Responders
NSF Latency (s)
800
600
400
200
0
0
50
100
150
200
Open Arm Time (s)

bioRxiv preprint doi: https://doi.org/10.1101/491613; this version posted December 10, 2018. The copyright holder for this preprint (which was not certified by peer review) is the author/funder. All rights reserved. No reuse allowed without permission.

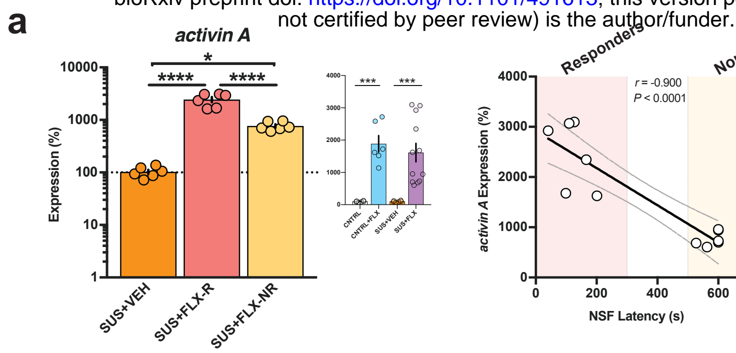

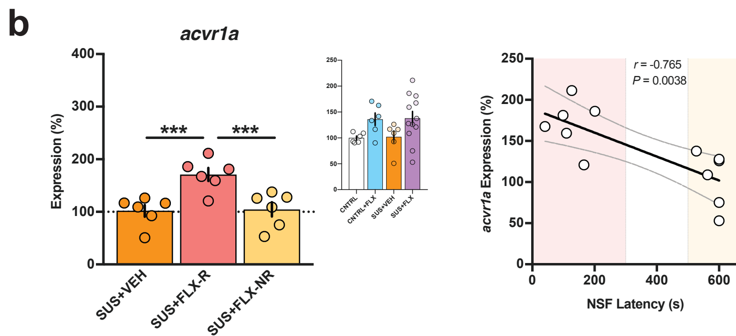

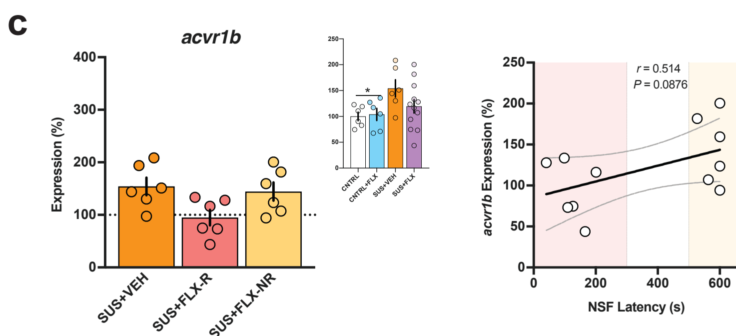

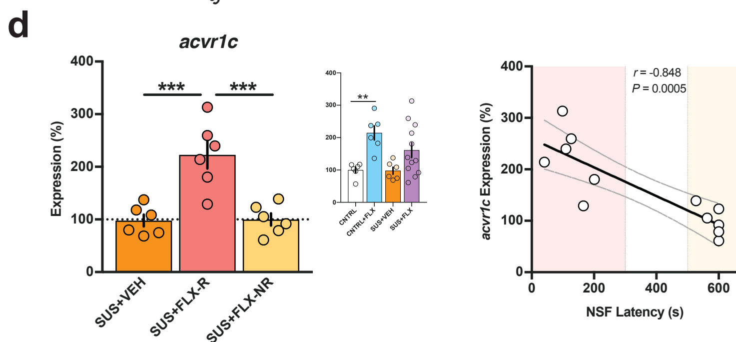

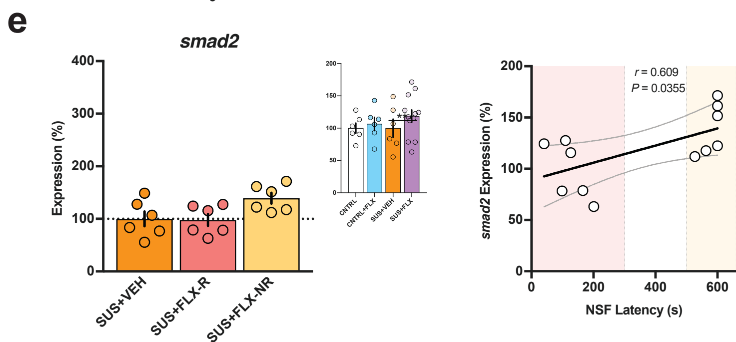

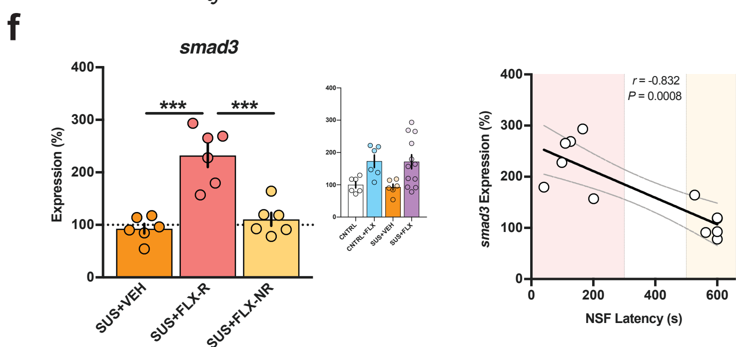

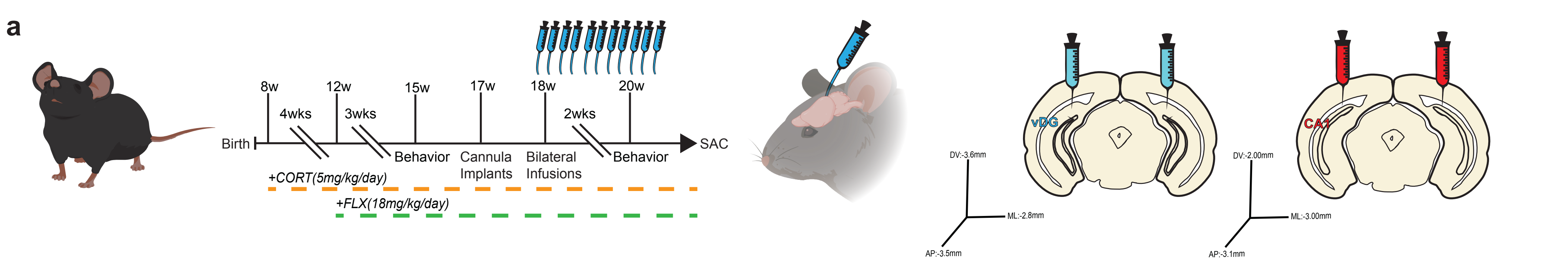
a
Birth
8w
4wks
12w
3wks
15w
Behavior
17w
Cannula
Implants
18w
Bilateral
Infusions
2wks
20w
Behavior
SAC
+CORT(5mg/kg/day)
+FLX(18mg/kg/day)
vDG
CA1

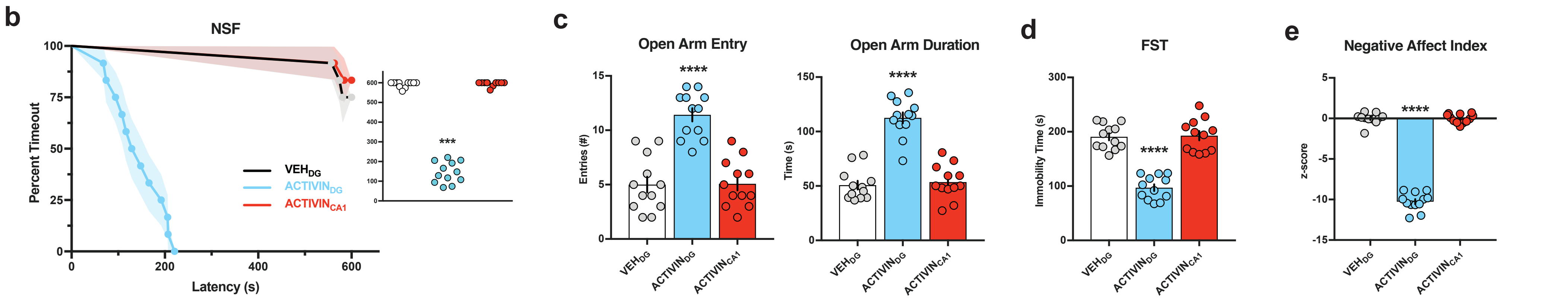
b
NSF
Percent Timeout
Latency (s)
VEH_DG
ACTIVIN_DG
ACTIVIN_CA1
***
c
Open Arm Entry
Entries (#)
****
Open Arm Duration
Time (s)
****
d
FST
Immobility Time (s)
****
e
Negative Affect Index
z-score
****

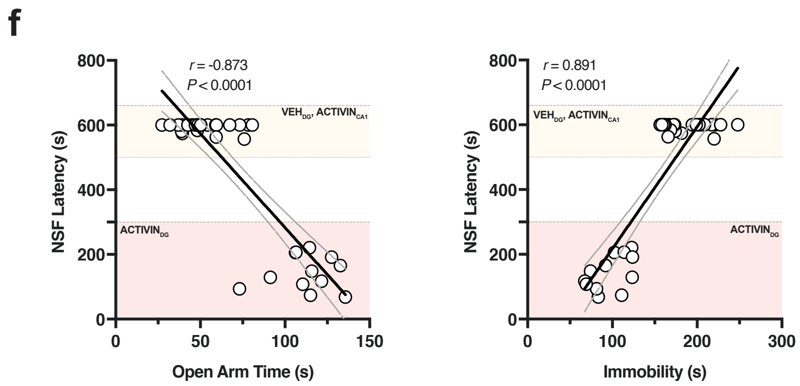
f
r = -0.873
P < 0.0001
NSF Latency (s)
Open Arm Time (s)
r = 0.891
P < 0.0001
Immobility (s)

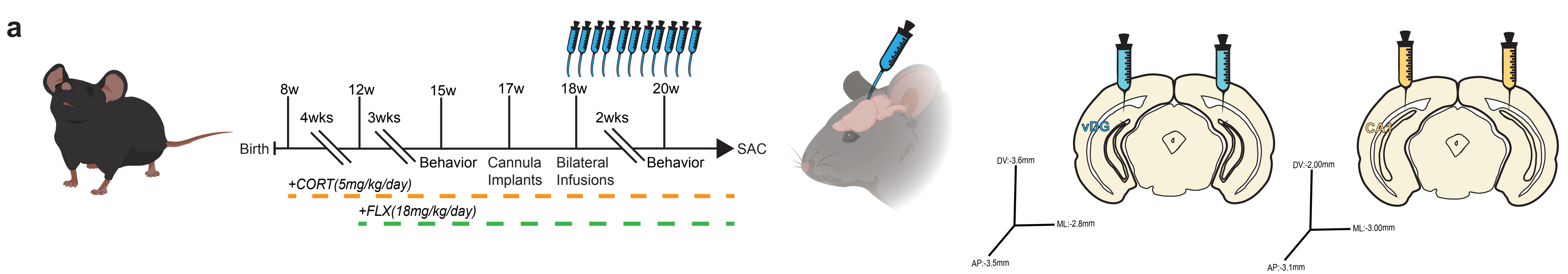
a
8w
12w
15w
17w
18w
20w
4wks
3wks
2wks
Birth
Behavior
Cannula Implants
Bilateral Infusions
Behavior
SAC
+CORT(5mg/kg/day)
+FLX(18mg/kg/day)
vDG
CA1
DV:-3.6mm
ML:-2.8mm
AP:-3.5mm
DV:-2.00mm
ML:-3.00mm
AP:-3.1mm

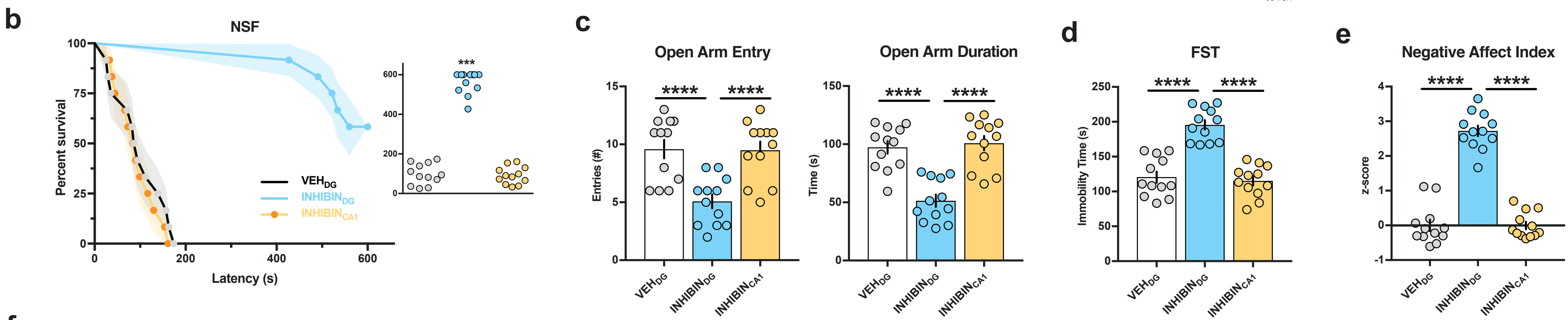
b
NSF
Percent survival
Latency (s)
VEH$_{DG}$
INHIBIN$_{DG}$
INHIBIN$_{CA1}$
***
c
Open Arm Entry
Entries (#)
****
Open Arm Duration
Time (s)
d
FST
Immobility Time (s)
e
Negative Affect Index
z-score
VEH$_{DG}$
INHIBIN$_{DG}$
INHIBIN$_{CA1}$

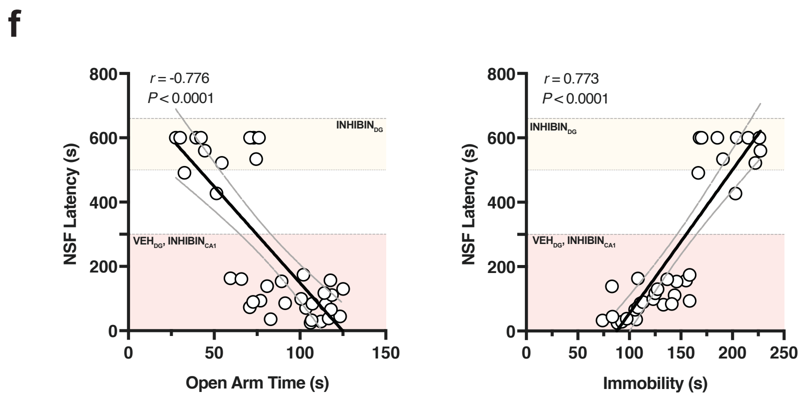
f
r = -0.776
P < 0.0001
NSF Latency (s)
Open Arm Time (s)
INHIBIN$_{DG}$
VEH$_{DG}$, INHIBIN$_{CA1}$
r = 0.773
P < 0.0001
Immobility (s)

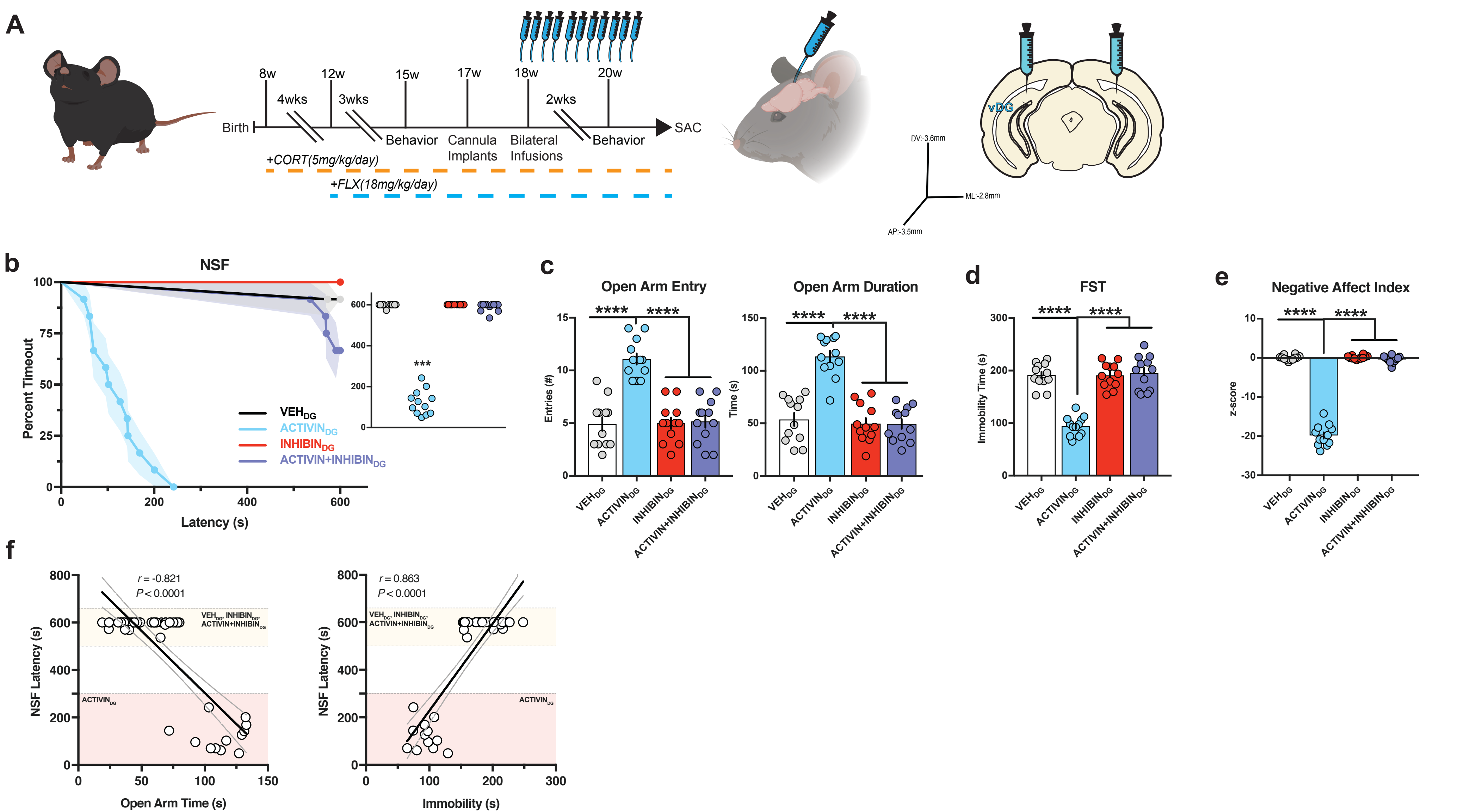
A
Birth
8w
4wks
12w
3wks
15w
Behavior
17w
Cannula Implants
18w
Bilateral Infusions
2wks
20w
Behavior
SAC
+CORT(5mg/kg/day)
+FLX(18mg/kg/day)
vDG
DV:-3.6mm
ML:-2.8mm
AP:-3.5mm
b
NSF
Percent Timeout
Latency (s)
VEH_DG
ACTIVIN_DG
INHIBIN_DG
ACTIVIN+INHIBIN_DG
***
c
Open Arm Entry
Entries (#)
Open Arm Duration
Time (s)
d
FST
Immobility Time (s)
e
Negative Affect Index
z-score
f
r = -0.821
P < 0.0001
r = 0.863
P < 0.0001
NSF Latency (s)
Open Arm Time (s)
Immobility (s)
VEH_DG, INHIBIN_DG, ACTIVIN+INHIBIN_DG
ACTIVIN_DG

bioRxiv preprint doi: https://doi.org/10.1101/491613; this version posted December 10, 2018. The copyright holder for this preprint (which was not certified by peer review) is the author/funder. All rights reserved. No reuse allowed without permission.

a

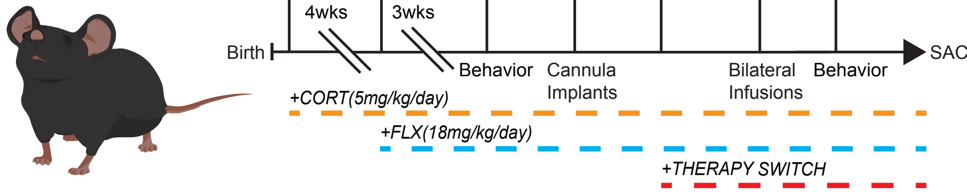

b

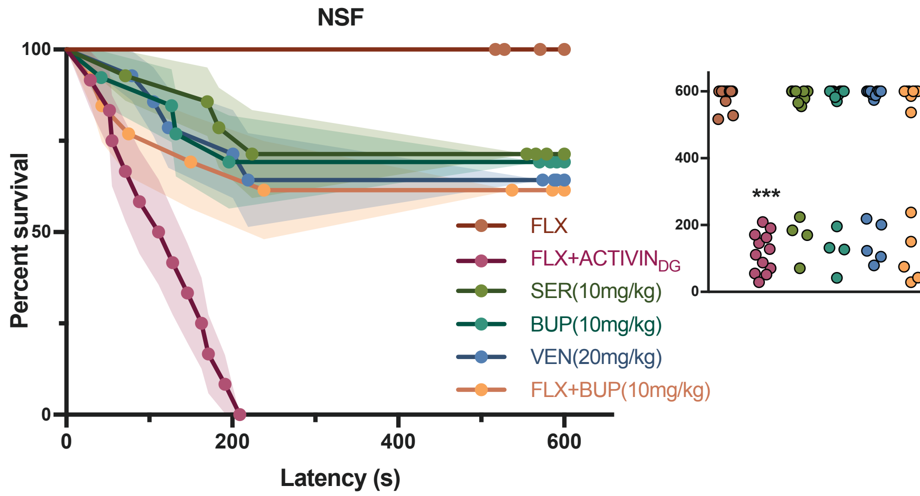

c

bioRxiv preprint doi: https://doi.org/10.1101/491613; this version posted December 10, 2018. The copyright holder for this preprint (which was not certified by peer review) is the author/funder. All rights reserved. No reuse allowed without permission.

a

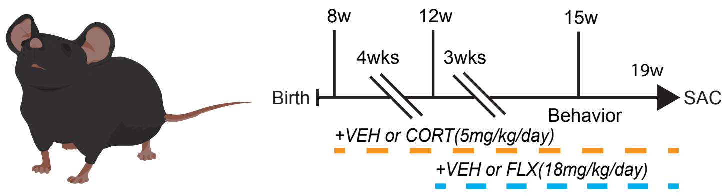

b

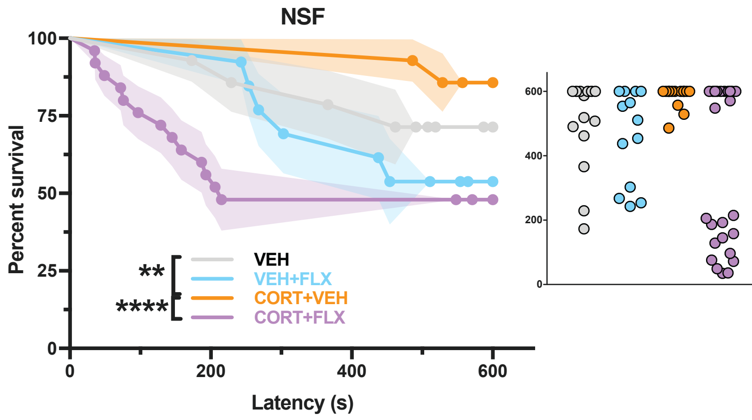

c

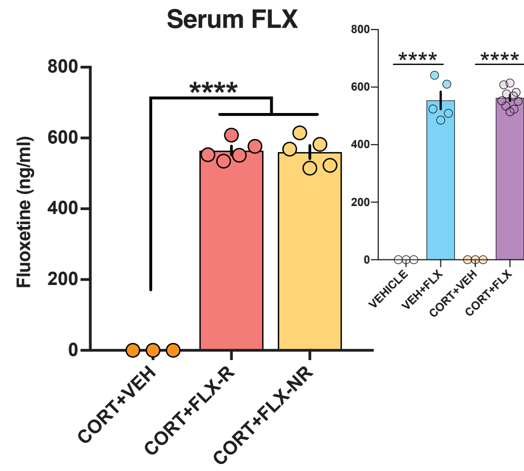

bioRxiv preprint doi: https://doi.org/10.1101/491613; this version posted December 10, 2018. The copyright holder for this preprint (which was not certified by peer review) is the author/funder. All rights reserved. No reuse allowed without permission.

a

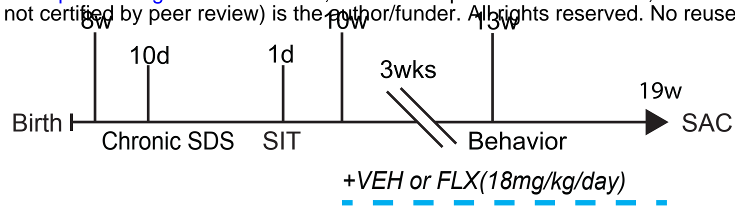

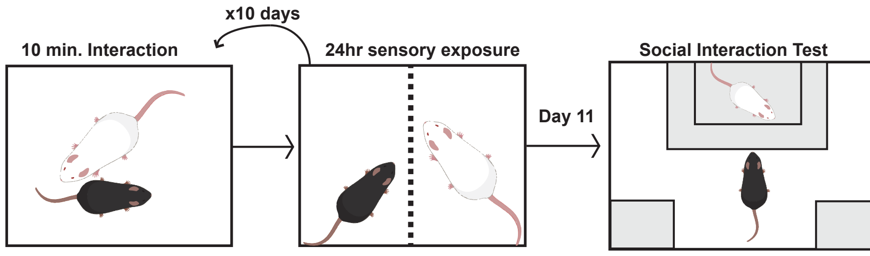

b

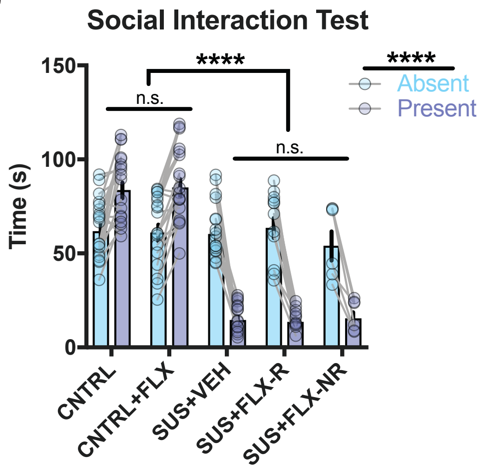

c